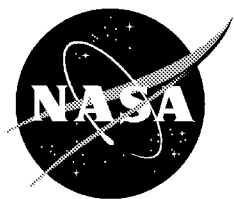


NASA/TM-2000-209026



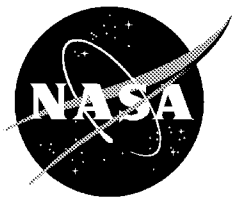
# 1999 Research Engineering Annual Report

*Compiled by  
Edmund Hamlin, Everlyn Cruciani, and Patricia Pearson  
NASA Dryden Flight Research Center  
Edwards, California*

---

**August 2000**

NASA/TM-2000-209026



# 1999 Research Engineering Annual Report

*Compiled by  
Edmund Hamlin, Everlyn Cruciani, and Patricia Pearson  
NASA Dryden Flight Research Center  
Edwards, California*

---

**August 2000**

## The NASA STI Program Office...in Profile

Since its founding, NASA has been dedicated to the advancement of aeronautics and space science. The NASA Scientific and Technical Information (STI) Program Office plays a key part in helping NASA maintain this important role.

The NASA STI Program Office is operated by Langley Research Center, the lead center for NASA's scientific and technical information. The NASA STI Program Office provides access to the NASA STI Database, the largest collection of aeronautical and space science STI in the world. The Program Office is also NASA's institutional mechanism for disseminating the results of its research and development activities. These results are published by NASA in the NASA STI Report Series, which includes the following report types:

- **TECHNICAL PUBLICATION.** Reports of completed research or a major significant phase of research that present the results of NASA programs and include extensive data or theoretical analysis. Includes compilations of significant scientific and technical data and information deemed to be of continuing reference value. NASA's counterpart of peer-reviewed formal professional papers but has less stringent limitations on manuscript length and extent of graphic presentations.
- **TECHNICAL MEMORANDUM.** Scientific and technical findings that are preliminary or of specialized interest, e.g., quick release reports, working papers, and bibliographies that contain minimal annotation. Does not contain extensive analysis.
- **CONTRACTOR REPORT.** Scientific and technical findings by NASA-sponsored contractors and grantees.
- **CONFERENCE PUBLICATION.** Collected papers from scientific and technical conferences, symposia, seminars, or other meetings sponsored or cosponsored by NASA.
- **SPECIAL PUBLICATION.** Scientific, technical, or historical information from NASA programs, projects, and mission, often concerned with subjects having substantial public interest.
- **TECHNICAL TRANSLATION.** English-language translations of foreign scientific and technical material pertinent to NASA's mission.

Specialized services that complement the STI Program Office's diverse offerings include creating custom thesauri, building customized databases, organizing and publishing research results...even providing videos.

For more information about the NASA STI Program Office, see the following:

- Access the NASA STI Program Home Page at <http://www.sti.nasa.gov>
- E-mail your question via the Internet to [help@sti.nasa.gov](mailto:help@sti.nasa.gov)
- Fax your question to the NASA Access Help Desk at (301) 621-0134
- Telephone the NASA Access Help Desk at (301) 621-0390
- Write to:  
NASA Access Help Desk  
NASA Center for AeroSpace Information  
7121 Standard Drive  
Hanover, MD 21076-1320

## The NASA STI Program Office...in Profile

Since its founding, NASA has been dedicated to the advancement of aeronautics and space science. The NASA Scientific and Technical Information (STI) Program Office plays a key part in helping NASA maintain this important role.

The NASA STI Program Office is operated by Langley Research Center, the lead center for NASA's scientific and technical information. The NASA STI Program Office provides access to the NASA STI Database, the largest collection of aeronautical and space science STI in the world. The Program Office is also NASA's institutional mechanism for disseminating the results of its research and development activities. These results are published by NASA in the NASA STI Report Series, which includes the following report types:

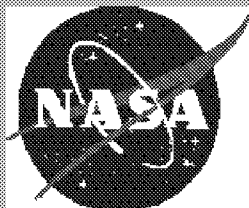
- **TECHNICAL PUBLICATION.** Reports of completed research or a major significant phase of research that present the results of NASA programs and include extensive data or theoretical analysis. Includes compilations of significant scientific and technical data and information deemed to be of continuing reference value. NASA's counterpart of peer-reviewed formal professional papers but has less stringent limitations on manuscript length and extent of graphic presentations.
- **TECHNICAL MEMORANDUM.** Scientific and technical findings that are preliminary or of specialized interest, e.g., quick release reports, working papers, and bibliographies that contain minimal annotation. Does not contain extensive analysis.
- **CONTRACTOR REPORT.** Scientific and technical findings by NASA-sponsored contractors and grantees.
- **CONFERENCE PUBLICATION.** Collected papers from scientific and technical conferences, symposia, seminars, or other meetings sponsored or cosponsored by NASA.
- **SPECIAL PUBLICATION.** Scientific, technical, or historical information from NASA programs, projects, and mission, often concerned with subjects having substantial public interest.
- **TECHNICAL TRANSLATION.** English-language translations of foreign scientific and technical material pertinent to NASA's mission.

Specialized services that complement the STI Program Office's diverse offerings include creating custom thesauri, building customized databases, organizing and publishing research results...even providing videos.

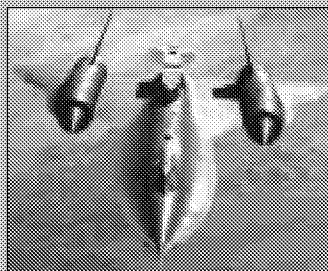
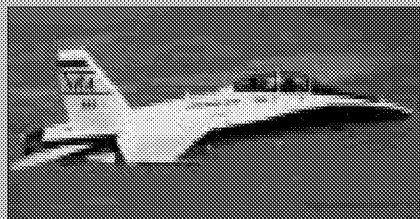
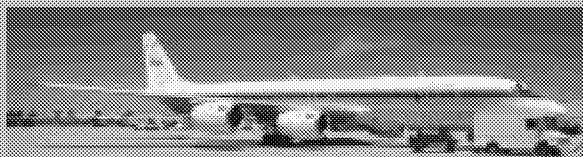
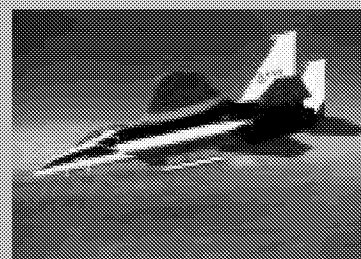
For more information about the NASA STI Program Office, see the following:

- Access the NASA STI Program Home Page at <http://www.sti.nasa.gov>
- E-mail your question via the Internet to [help@sti.nasa.gov](mailto:help@sti.nasa.gov)
- Fax your question to the NASA Access Help Desk at (301) 621-0134
- Telephone the NASA Access Help Desk at (301) 621-0390
- Write to:  
NASA Access Help Desk  
NASA Center for AeroSpace Information  
7121 Standard Drive  
Hanover, MD 21076-1320

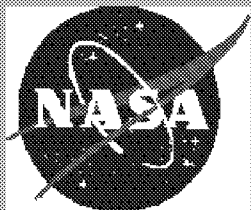




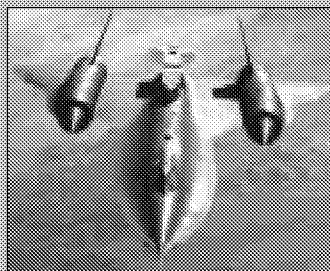
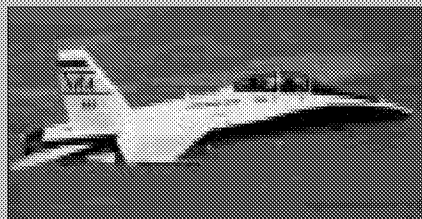
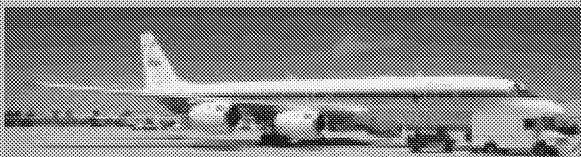
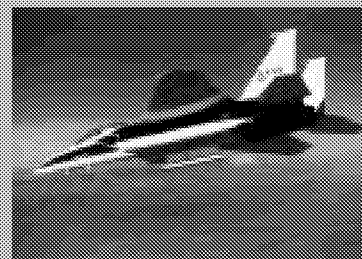
## NASA Dryden Flight Research Center Edwards, California



## 1999 Research Engineering Annual Report



## NASA Dryden Flight Research Center Edwards, California



## 1999 Research Engineering Annual Report

## NOTICE

Use of trade names or names of manufacturers in this document does not constitute an official endorsement of such products or manufacturers, either expressed or implied, by the National Aeronautics and Space Administration.

Available from the following:

NASA Center for AeroSpace Information (CASI)  
7121 Standard Drive  
Hanover, MD 21076-1320  
(301) 621-0390

National Technical Information Service (NTIS)  
5285 Port Royal Road  
Springfield, VA 22161-2171  
(703) 487-4650

## NOTICE

Use of trade names or names of manufacturers in this document does not constitute an official endorsement of such products or manufacturers, either expressed or implied, by the National Aeronautics and Space Administration.

Available from the following:

NASA Center for AeroSpace Information (CASI)  
7121 Standard Drive  
Hanover, MD 21076-1320  
(301) 621-0390

National Technical Information Service (NTIS)  
5285 Port Royal Road  
Springfield, VA 22161-2171  
(703) 487-4650

# 1999 Research Engineering Report

## Table of Contents

<u>Title</u>	<u>First Author</u>	<u>Page</u>
Preface	Robert Meyer	v
Research Engineering Directorate R		
Organizational Chart		vi
Research Engineering Directorate Staff		vii
Supersonic Natural Laminar Flow Flight Research	Daniel W. Banks	1
Infrared Flight Test Techniques	Daniel W. Banks	2
HAVE RECKON Project	Alex Sim	3
Mars Airplane Entry, Descent and Flight		
Trajectory Development	James Murray	4
Blunt Body Drag Reduction Using Forebody		
Surface Roughness	Stephen A. Whitmore	5
DC-8 Reduced Vertical Separation Minimum (RVSM)		
Certification	Edward A. Haering, Jr.	8
F-18 Stability and Control Derivative Estimation		
for Active Aeroelastic Wing Risk Reduction	Tim Moes	9
SR-71 Testbed Configuration Envelope Expansion	Tim Moes	10
Flight Test of a Gripen Ministick Controller in an		
F/A-18 Aircraft	Patrick C. Stoliker	11
Autopilot Design for Autonomous Recovery of the APEX		
Remotely Piloted Vehicle (RPV)	Marle Hewett	12
AAW Risk Reduction Flights Using the PSFCC Computers	John Carter	13
X-33 Avionics Integration & Real-time Nonlinear Simulation	Bob Clarke	14
X-33 Landing Gear Dynamics Model	Louis Lintereur	15
X-43A Non-Linear Monte Carlo Analysis	Ethan Baumann	16
Unmanned Combat Air Vehicle	Neil Matheny	17
X-43A Hypersonic Blended Inertial and Pneumatic		
Angle of Attack	Joe Pahle	18
F/A-18 Autonomous Formation Flight	Curtis E. Hanson	19
F/A-18B Systems Research Aircraft (SRA) X-33 Vehicle		
Health Monitoring System Risk Reduction Experiment	Keith Schweikhard	20
Flight Test of an Intelligent Flight Control System on the		
F-15 ACTIVE	Michael P. Thomson	21
X-Actuator Control Test (X-ACT) Program	Stephen Jensen	22
X-43A Antenna Patterns	Mark W. Hodge	23
Reconfigurable VHF Broadcast Differential GPS Base Station	Glenn Bever	24
DSP/GEDAE Signal Processing Algorithms	Arild Bertelrud	25
Multiplexed Hot Films	Arild Bertelrud	26
LABVIEW Based ESP Pressure Data Acquisition System	Alma M. Warner	27

# 1999 Research Engineering Report

## Table of Contents

<u>Title</u>	<u>First Author</u>	<u>Page</u>
Preface	Robert Meyer	v
Research Engineering Directorate R		
Organizational Chart		vi
Research Engineering Directorate Staff		vii
Supersonic Natural Laminar Flow Flight Research	Daniel W. Banks	1
Infrared Flight Test Techniques	Daniel W. Banks	2
HAVE RECKON Project	Alex Sim	3
Mars Airplane Entry, Descent and Flight		
Trajectory Development	James Murray	4
Blunt Body Drag Reduction Using Forebody		
Surface Roughness	Stephen A. Whitmore	5
DC-8 Reduced Vertical Separation Minimum (RVSM)		
Certification	Edward A. Haering, Jr.	8
F-18 Stability and Control Derivative Estimation		
for Active Aeroelastic Wing Risk Reduction	Tim Moes	9
SR-71 Testbed Configuration Envelope Expansion	Tim Moes	10
Flight Test of a Gripen Ministick Controller in an		
F/A-18 Aircraft	Patrick C. Stoliker	11
Autopilot Design for Autonomous Recovery of the APEX		
Remotely Piloted Vehicle (RPV)	Marle Hewett	12
AAW Risk Reduction Flights Using the PSFCC Computers	John Carter	13
X-33 Avionics Integration & Real-time Nonlinear Simulation	Bob Clarke	14
X-33 Landing Gear Dynamics Model	Louis Lintereur	15
X-43A Non-Linear Monte Carlo Analysis	Ethan Baumann	16
Unmanned Combat Air Vehicle	Neil Matheny	17
X-43A Hypersonic Blended Inertial and Pneumatic		
Angle of Attack	Joe Pahle	18
F/A-18 Autonomous Formation Flight	Curtis E. Hanson	19
F/A-18B Systems Research Aircraft (SRA) X-33 Vehicle		
Health Monitoring System Risk Reduction Experiment	Keith Schweikhard	20
Flight Test of an Intelligent Flight Control System on the		
F-15 ACTIVE	Michael P. Thomson	21
X-Actuator Control Test (X-ACT) Program	Stephen Jensen	22
X-43A Antenna Patterns	Mark W. Hodge	23
Reconfigurable VHF Broadcast Differential GPS Base Station	Glenn Bever	24
DSP/GEDAE Signal Processing Algorithms	Arild Bertelrud	25
Multiplexed Hot Films	Arild Bertelrud	26
LABVIEW Based ESP Pressure Data Acquisition System	Alma M. Warner	27

Flight Instrumentation for X-33 Extended Range Test	Terry Montgomery	28
Efficient Modulation Techniques	Don Whiteman	29
X-43A Flight Research Plans Overview	Griff Corpening	30
X-43 Fluid Systems Development	Masashi Mizukami	31
X-43A Environmental Control Systems Performance	Neal Hass	32
Advances in Leak Detection Technologies	Neal Hass	33
Hyper-X Propulsion Flight Research Plans	Ross Hathaway	34
Development of Scramjet Skin Friction Gages	Trong Bui	35
Gust Monitoring and Aeroelasticity Experiment	Stephen Corda	36
F-15B Propulsion Flight Test Fixture (P-FTF)	Jake Vachon	37
F-15 Skin Friction Flight Test	Trong Bui	38
X-43A Propulsion System Controls Update	John Orme	39
Development of Remote Site Capability for Flight Research	Lawrence C. Freudinger	40
AeroSAPIENT Project Initiated	Lawrence C. Freudinger	41
Integration of Finite Element Analysis Predicted Strains with a Strain Gage Loads Equation Derivation Package	Clifford D. Sticht	42
Non-Invasive In-Flight Structural Deflection Measurement	William A. Lokos	43
Aerostructures Test Wing	David F. Voracek	44
Blackbody Lightpipe Temperature Sensor Development	Larry Hudson	45
Spaceliner 100 Carbon-Carbon Control Surface Test Program	Larry Hudson	46
Radiant Heat Flux Gage Calibration System Characterization	Thomas J. Horn	47
Thermostructural Analysis of Superalloy Thermal Protection System (TPS)	Dr. William L. Ko	48
Validation of the Baseline F-18 Loads Model Using F-18/SRA Parameter Identification Flight Data	DiDi Olney	49
PC Based Thermal Control System	Alphonzo J. Stewart	50
Robust Control Design for the F/A-18 Active Aeroelastic Wing	Rick Lind	51
Application of Gain-Scheduled, Multivariable Control Techniques to the F/A-18 PSFCC	Mark Stephenson	52
Fiber Optic Instrumentation Development	Lance Richards	53
1999 Technical Publications		54
Tech Briefs, Patents, and Space Act Awards, FY 99		60

Flight Instrumentation for X-33 Extended Range Test	Terry Montgomery	28
Efficient Modulation Techniques	Don Whiteman	29
X-43A Flight Research Plans Overview	Griff Corpening	30
X-43 Fluid Systems Development	Masashi Mizukami	31
X-43A Environmental Control Systems Performance	Neal Hass	32
Advances in Leak Detection Technologies	Neal Hass	33
Hyper-X Propulsion Flight Research Plans	Ross Hathaway	34
Development of Scramjet Skin Friction Gages	Trong Bui	35
Gust Monitoring and Aeroelasticity Experiment	Stephen Corda	36
F-15B Propulsion Flight Test Fixture (P-FTF)	Jake Vachon	37
F-15 Skin Friction Flight Test	Trong Bui	38
X-43A Propulsion System Controls Update	John Orme	39
Development of Remote Site Capability for Flight Research	Lawrence C. Freudinger	40
AeroSAPIENT Project Initiated	Lawrence C. Freudinger	41
Integration of Finite Element Analysis Predicted Strains with a Strain Gage Loads Equation Derivation Package	Clifford D. Sticht	42
Non-Invasive In-Flight Structural Deflection Measurement	William A. Lokos	43
Aerostructures Test Wing	David F. Voracek	44
Blackbody Lightpipe Temperature Sensor Development	Larry Hudson	45
Spaceliner 100 Carbon-Carbon Control Surface Test Program	Larry Hudson	46
Radiant Heat Flux Gage Calibration System Characterization	Thomas J. Horn	47
Thermostructural Analysis of Superalloy Thermal Protection System (TPS)	Dr. William L. Ko	48
Validation of the Baseline F-18 Loads Model Using F-18/SRA Parameter Identification Flight Data	DiDi Olney	49
PC Based Thermal Control System	Alphonzo J. Stewart	50
Robust Control Design for the F/A-18 Active Aeroelastic Wing	Rick Lind	51
Application of Gain-Scheduled, Multivariable Control Techniques to the F/A-18 PSFCC	Mark Stephenson	52
Fiber Optic Instrumentation Development	Lance Richards	53
1999 Technical Publications		54
Tech Briefs, Patents, and Space Act Awards, FY 99		60



## *Preface*

The NASA Dryden Flight Research Center's Research Engineering Directorate is a diverse and broad-based organization composed of the many disciplinary skills required to successfully conduct flight research. The directorate is comprised of six branches representing the principal disciplines of: Aerodynamics, Dynamics and Controls, Flight Systems, Flight Instrumentation, Propulsion and Performance, and Aerostructures. The Directorate organization is illustrated on the chart following this page.

We are very proud of the many significant accomplishments of our technical staff during the calendar year 1999. These milestones include both those accomplished in support of research programs as well as basic research performed within the Directorate, supported by our competitively-funded Flight Test Techniques and Disciplinary Flight Research programs.

This Annual Report encompasses the full range of research accomplishments, from the project level, flight test techniques, to disciplinary flight research programs. It includes one-page summaries of each program; more details are available from the principal investigators as noted on the summaries. There are also included a list of the many technical publications completed in the last year, from in-house, university, and contract researchers under the auspices of the Directorate.

Calendar year 2000 promises to be an even more productive year, with a mix of new and continuing research programs. I look forward to reporting on these efforts next year.



R.R. Meyer

Director of Research Engineering  
Dryden Flight Research Center

## *Preface*

The NASA Dryden Flight Research Center's Research Engineering Directorate is a diverse and broad-based organization composed of the many disciplinary skills required to successfully conduct flight research. The directorate is comprised of six branches representing the principal disciplines of: Aerodynamics, Dynamics and Controls, Flight Systems, Flight Instrumentation, Propulsion and Performance, and Aerostructures. The Directorate organization is illustrated on the chart following this page.

We are very proud of the many significant accomplishments of our technical staff during the calendar year 1999. These milestones include both those accomplished in support of research programs as well as basic research performed within the Directorate, supported by our competitively-funded Flight Test Techniques and Disciplinary Flight Research programs.

This Annual Report encompasses the full range of research accomplishments, from the project level, flight test techniques, to disciplinary flight research programs. It includes one-page summaries of each program; more details are available from the principal investigators as noted on the summaries. There are also included a list of the many technical publications completed in the last year, from in-house, university, and contract researchers under the auspices of the Directorate.

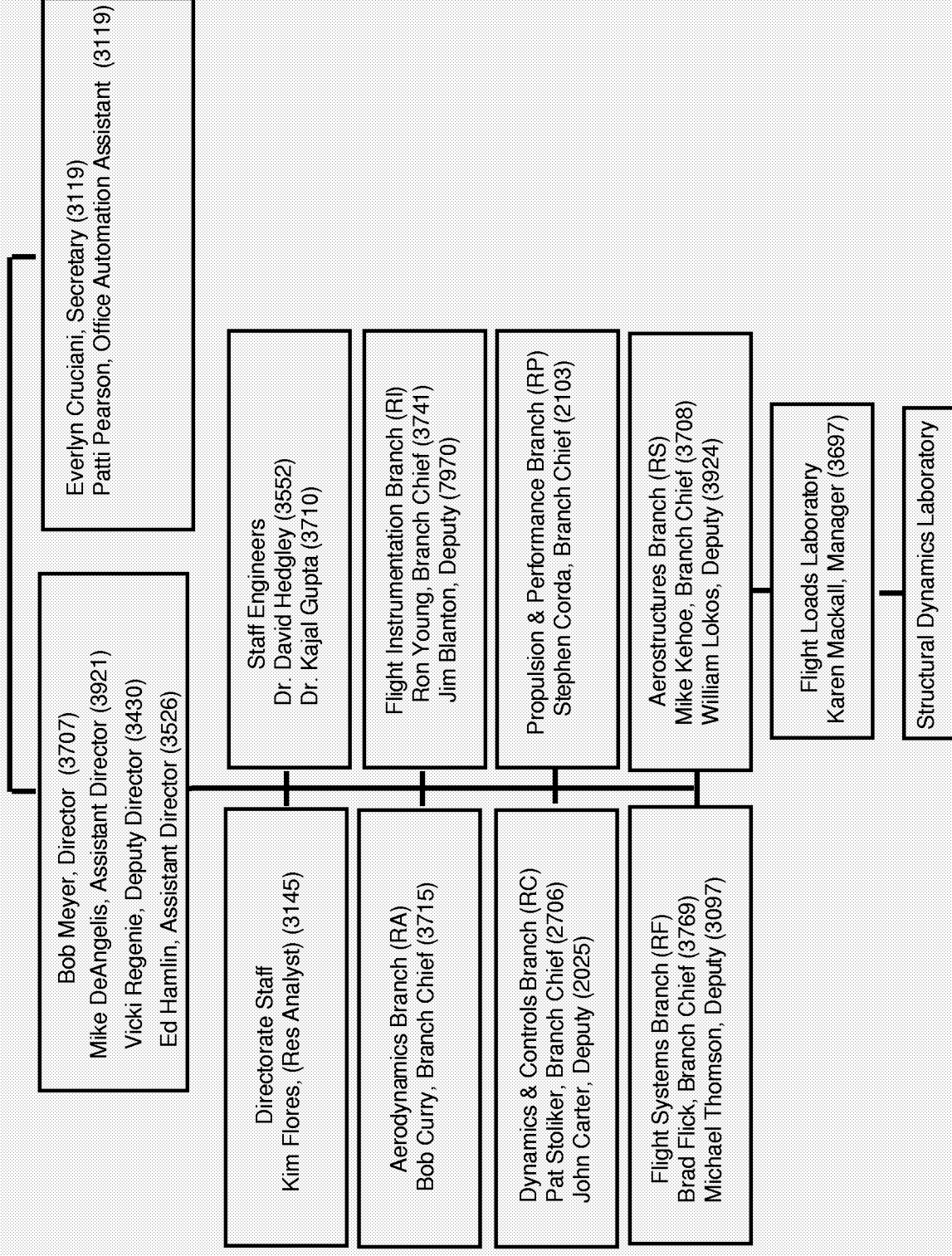
Calendar year 2000 promises to be an even more productive year, with a mix of new and continuing research programs. I look forward to reporting on these efforts next year.



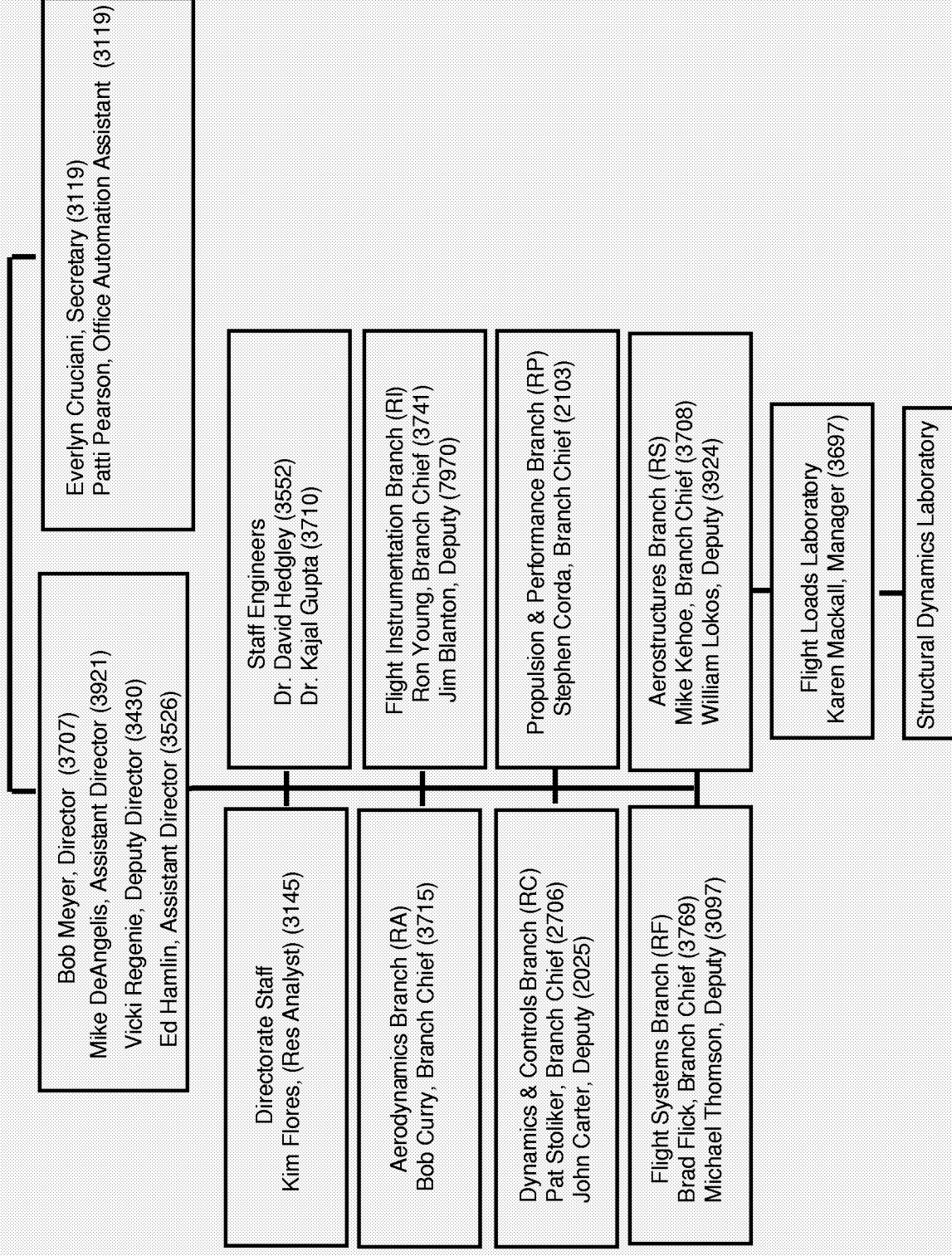
R.R. Meyer

Director of Research Engineering  
Dryden Flight Research Center

# Research Engineering Directorate (R)



# Research Engineering Directorate (R)



## **Research Engineering Directorate Staff**

Director	Robert R. Meyer, Jr.
Deputy Director	Victoria A. Regenie
Assistant Director	Michael DeAngelis
Assistant Director	Edmund M. Hamlin
Secretary	Everlyn Y. Cruciani

### **Branch Codes and Chiefs**

RA – Aerodynamics	Robert E. Curry
RC – Dynamics and Controls	Patrick C. Stoliker
RF – Flight Systems	Bradley C. Flick
RI – Flight Instrumentation	Ronald Young
RP – Propulsion and Performance	Stephen Corda
RS – Aerostructures	Michael W. Kehoe

## **Research Engineering Directorate Staff**

Director	Robert R. Meyer, Jr.
Deputy Director	Victoria A. Regenie
Assistant Director	Michael DeAngelis
Assistant Director	Edmund M. Hamlin
Secretary	Everlyn Y. Cruciani

### **Branch Codes and Chiefs**

RA – Aerodynamics	Robert E. Curry
RC – Dynamics and Controls	Patrick C. Stoliker
RF – Flight Systems	Bradley C. Flick
RI – Flight Instrumentation	Ronald Young
RP – Propulsion and Performance	Stephen Corda
RS – Aerostructures	Michael W. Kehoe

# Supersonic Natural Laminar Flow Flight Research

## Summary

Airfoil designs capable of passively maintaining laminar flow at supersonic speeds have been shown by theory and small scale tests. Recent flight tests now prove that these designs can maintain large runs of laminar flow at higher Reynolds numbers in a harsh flight environment. Laminar flow was measured using a commercially available infrared detector adapted for flight. These tests were performed on the Dryden F-15B aircraft.

## Objective

- Acquire IR images of natural laminar flow up to  $M=2.0$ .
- Obtain large runs of laminar flow at highest unit Reynolds number possible with F-15B aircraft.
- Determine conditions where laminar flow breaks down.

## Approach

Using an aircraft mounted infrared camera, laminar flow was measured on a test article mounted on the centerline pylon of an F-15B aircraft. The IR camera measures surface temperatures which change with the different boundary layer states. The surface beneath the turbulent boundary layer will be warmer than that beneath the laminar layer due to the higher convection of the turbulent layer with the freestream. The laminar flow, for these conditions, will be darker and the turbulent flow lighter.

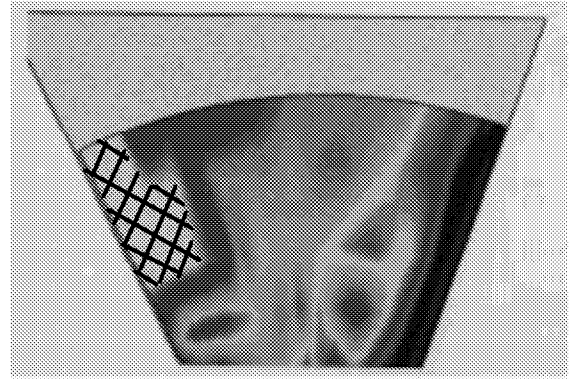
The test article was fabricated from aluminum with an insulating layer covering all but the first 1 to 2 inches of the leading and trailing edges. A splitter plate was formed over the test wing to minimize disturbances from the bottom of the aircraft affecting the test surface.

## Results

Laminar flow was obtained up to full chord for the outer 1/3 span and approximately 80% of the inner 2/3. The laminar flow was able to penetrate weak shock waves, but was typically terminated by strong shock waves. The strongest shock wave appeared to emanate from the camera pod located outboard on the armament rail.

## Status/Plans

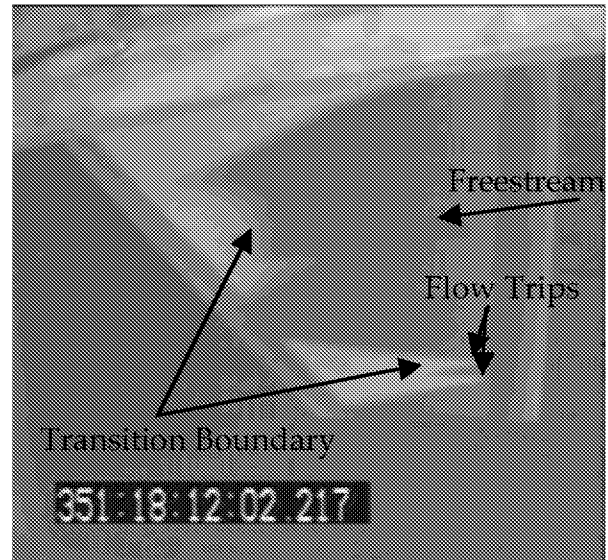
The next flights will assess cross-flow disturbances by flying with a 30 degree leading edge. Future flights will obtain more detailed data by instrumenting the test article with surface pressures and thermocouples. Also the data recording system will be updated to record the full digital images from the camera. A follow on program would increase the size of the test article and incorporate potential control surfaces to assess the effects of higher Reynolds numbers and systems issues.



Predicted transition pattern of test article  
(cross-hatched area denotes transition).



Supersonic Natural Laminar Flow test  
article mounted on F-15B aircraft.



Infrared image of Supersonic Natural  
Laminar Flow test fixture.

## Contact:

Daniel W. Banks, DFRC, RA

(661) 258-2921 dan.banks@dfrc.nasa.gov

# Supersonic Natural Laminar Flow Flight Research

## Summary

Airfoil designs capable of passively maintaining laminar flow at supersonic speeds have been shown by theory and small scale tests. Recent flight tests now prove that these designs can maintain large runs of laminar flow at higher Reynolds numbers in a harsh flight environment. Laminar flow was measured using a commercially available infrared detector adapted for flight. These tests were performed on the Dryden F-15B aircraft.

## Objective

- Acquire IR images of natural laminar flow up to  $M=2.0$ .
- Obtain large runs of laminar flow at highest unit Reynolds number possible with F-15B aircraft.
- Determine conditions where laminar flow breaks down.

## Approach

Using an aircraft mounted infrared camera, laminar flow was measured on a test article mounted on the centerline pylon of an F-15B aircraft. The IR camera measures surface temperatures which change with the different boundary layer states. The surface beneath the turbulent boundary layer will be warmer than that beneath the laminar layer due to the higher convection of the turbulent layer with the freestream. The laminar flow, for these conditions, will be darker and the turbulent flow lighter.

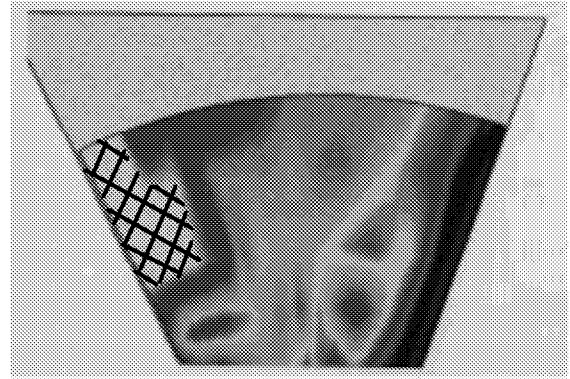
The test article was fabricated from aluminum with an insulating layer covering all but the first 1 to 2 inches of the leading and trailing edges. A splitter plate was formed over the test wing to minimize disturbances from the bottom of the aircraft affecting the test surface.

## Results

Laminar flow was obtained up to full chord for the outer 1/3 span and approximately 80% of the inner 2/3. The laminar flow was able to penetrate weak shock waves, but was typically terminated by strong shock waves. The strongest shock wave appeared to emanate from the camera pod located outboard on the armament rail.

## Status/Plans

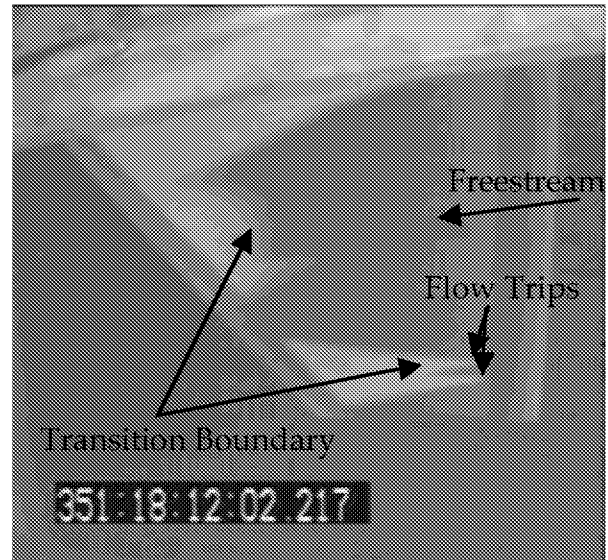
The next flights will assess cross-flow disturbances by flying with a 30 degree leading edge. Future flights will obtain more detailed data by instrumenting the test article with surface pressures and thermocouples. Also the data recording system will be updated to record the full digital images from the camera. A follow on program would increase the size of the test article and incorporate potential control surfaces to assess the effects of higher Reynolds numbers and systems issues.



Predicted transition pattern of test article  
(cross-hatched area denotes transition).



Supersonic Natural Laminar Flow test  
article mounted on F-15B aircraft.



Infrared image of Supersonic Natural  
Laminar Flow test fixture.

## Contact:

Daniel W. Banks, DFRC, RA

(661) 258-2921 [dan.banks@dfrc.nasa.gov](mailto:dan.banks@dfrc.nasa.gov)



# Infrared Flight Test Techniques

## Summary

Infrared thermography is a very powerful technique to both visualize and quantify flow fields over the speed range. It is both global and non-intrusive. It is most widely used in aerodynamic flight test to measure laminar/turbulent transition, but can also identify shocks and measure aeroheating. Three different techniques of acquiring the IR thermograms are employed. These are a fixed system on the aircraft to be visualized, a remote system on a second aircraft, and a ground based remote system employing long range optics. These systems and techniques have been used to visualize flow fields from subsonic to hypersonic speeds.

## Objectives

- Acquire infrared thermograms in flight.
- Process images for motion and spatial corrections, and enhancement.
- Calibrate and measure surface temperatures
- Identify and locate boundary layer transition, shock waves, and other flow phenomena.

## Approach

By using various IR systems and techniques flow field information has been acquired across the speed range. Remotely mounted aircraft systems have been used to acquire data from other unmodified aircraft in flight from subsonic through low supersonic speeds. Fixed systems have been used to measure test articles at supersonic speeds but are applicable for a variety of applications and speed ranges. Ground based remote imaging (Langley lead for this effort) has been developed for measuring transition and aeroheating of re-entering re-useable launch vehicles.

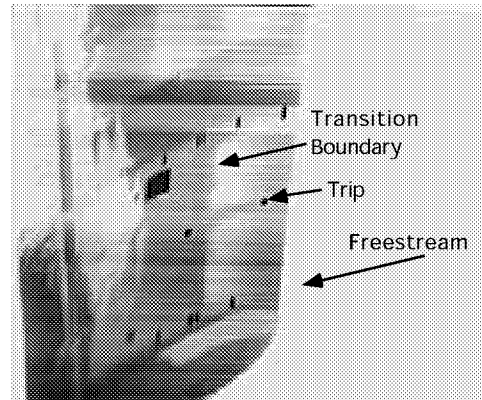
## Results

Excellent results have been obtained from each type of system and at each speed range. The ability to locate boundary layer transition, shock waves, and measure surface temperatures has been demonstrated.

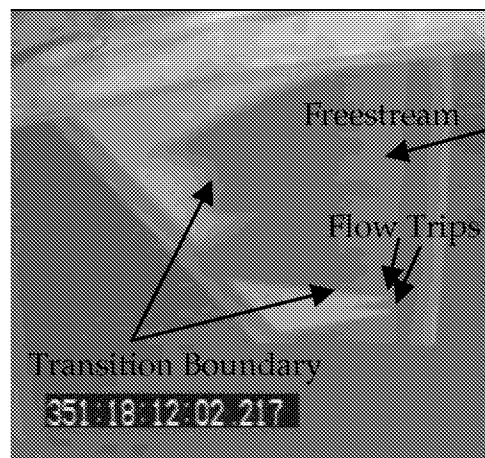
The top figure shows transition on a subsonic wing. The surface is heated by solar radiation so that the laminar regions are lighter in color. The middle figure shows transition on a supersonic laminar flow test article. In this case the surface is heated by the freestream, so the laminar areas are darker. The bottom figure shows the space shuttle on re-entry. In this case the lighter areas denote regions of higher surface heating (entire vehicle is turbulent).

## Status/Plans

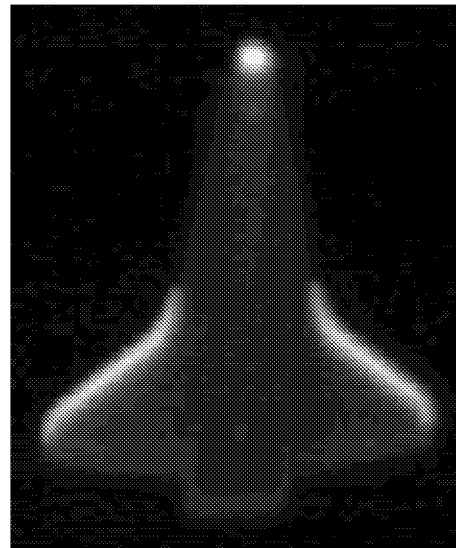
Continue developing infrared systems and techniques for flight research.



T-34 wing imaged remotely by F-18 FLIR.



Infrared image of supersonic natural laminar flow test fixture imaged with a fixed IR system.



Space shuttle STS-96 imaged with ground based IR.

## Contact

Daniel W. Banks, DFRC, RA, (661) 258-2921  
Robert C. Blanchard, LaRC

# Infrared Flight Test Techniques

## Summary

Infrared thermography is a very powerful technique to both visualize and quantify flow fields over the speed range. It is both global and non-intrusive. It is most widely used in aerodynamic flight test to measure laminar/turbulent transition, but can also identify shocks and measure aeroheating. Three different techniques of acquiring the IR thermograms are employed. These are a fixed system on the aircraft to be visualized, a remote system on a second aircraft, and a ground based remote system employing long range optics. These systems and techniques have been used to visualize flow fields from subsonic to hypersonic speeds.

## Objectives

- Acquire infrared thermograms in flight.
- Process images for motion and spatial corrections, and enhancement.
- Calibrate and measure surface temperatures
- Identify and locate boundary layer transition, shock waves, and other flow phenomena.

## Approach

By using various IR systems and techniques flow field information has been acquired across the speed range. Remotely mounted aircraft systems have been used to acquire data from other unmodified aircraft in flight from subsonic through low supersonic speeds. Fixed systems have been used to measure test articles at supersonic speeds but are applicable for a variety of applications and speed ranges. Ground based remote imaging (Langley lead for this effort) has been developed for measuring transition and aeroheating of re-entering re-useable launch vehicles.

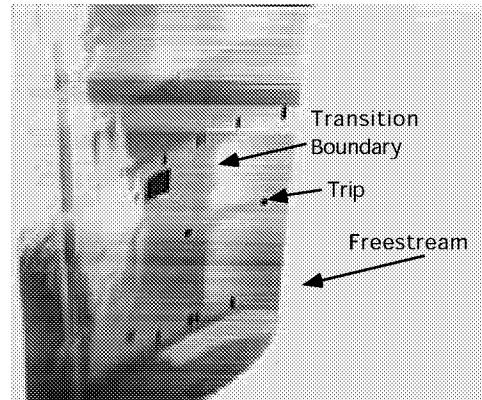
## Results

Excellent results have been obtained from each type of system and at each speed range. The ability to locate boundary layer transition, shock waves, and measure surface temperatures has been demonstrated.

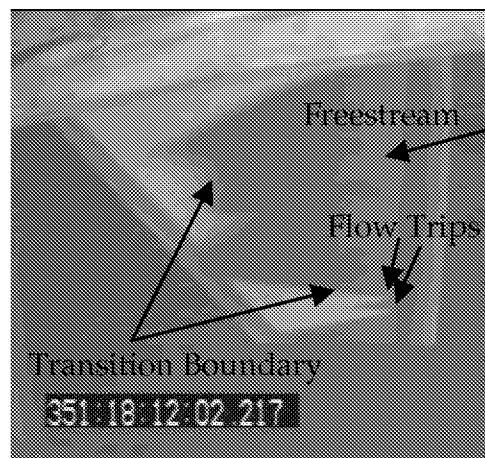
The top figure shows transition on a subsonic wing. The surface is heated by solar radiation so that the laminar regions are lighter in color. The middle figure shows transition on a supersonic laminar flow test article. In this case the surface is heated by the freestream, so the laminar areas are darker. The bottom figure shows the space shuttle on re-entry. In this case the lighter areas denote regions of higher surface heating (entire vehicle is turbulent).

## Status/Plans

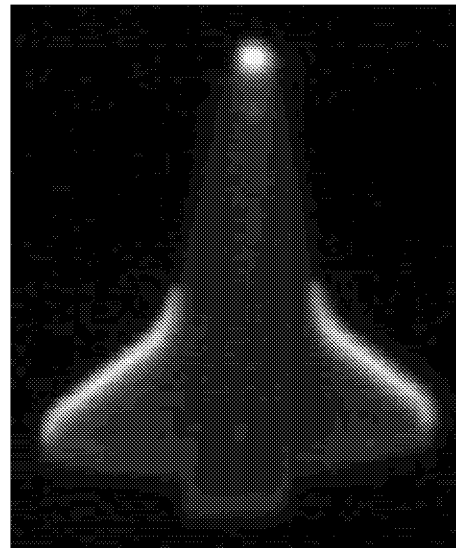
Continue developing infrared systems and techniques for flight research.



T-34 wing imaged remotely by F-18 FLIR.



Infrared image of supersonic natural laminar flow test fixture imaged with a fixed IR system.



Space shuttle STS-96 imaged with ground based IR.

## Contact

Daniel W. Banks, DFRC, RA, (661) 258-2921  
Robert C. Blanchard, LaRC

# HAVE RECKON Project

## Summary

When an Uninhabited Aerial Vehicle, UAV, is piloted from a ground control station, it is referred to as a Remotely Piloted Vehicle. A delay of typically 0.1 seconds is incurred as the vehicle processes the uplink signal and the vehicle response is prepared for downlink. When an RPV is flown over the horizon, the uplink and downlink signals still need to be relayed back to the ground station. A desirable relay is to use a satellite as the link. However a satellite link to the UAV and back often results in an additional signal transport delay of about 0.4 seconds. This 0.5 seconds total delay is enough to significantly degrade the handling qualities of an RPV. For a high-gain piloting task, this may even be enough lag to make the vehicle uncontrollable.

The USAF Test Pilot School, TPS, proposed to enhance the handling qualities by using a model-based predictive algorithm to compensate for system time delay. The algorithm would reside within the ground station and provide the ground pilot with predictive enhancements overlaid on the ground monitor. The compensation was functionally independent of the UAV. To conduct a low-cost flight research experiment, TPS contacted the Dryden Subscale Facility (model shop). Dryden agreed to provide the "UAV", safety pilot, ground cockpit, telemetry van and other lesser assets for the flight tests. The scope of the experiment was limited to the longitudinal axis.

## Objective

The USAF TPS general objective was to determine the improvement in UAV handling qualities when using a model-based predictive algorithm to compensate for system time delay. NASA Dryden's primary objectives were to provide the TPS with an aerodynamic model of the flight vehicle, integrate the vehicle systems, and safely conduct the flight tests.

## Results

Dryden chose a large utilitarian model, called the Mothership, that was capable of lifting 25 lbs of payload and still remain within the Dryden definition of a model airplane. A 16-channel data system was carried in a pod under the main fuselage. An airdata noseboom was mounted on the nose. A forward-looking video camera was installed in a pod above the wing. Measurements of elevator, pitch rate, and angle of attack were downlinked on the audio channel of the video signal. A telemetry van was used to separate the data from the audio channel and put it onto an ethernet line to an USAF Unix workstation next to the research cockpit. The workstation generated the transport lag by passing a delayed video frame to the monitor. The workstation was also used to generate the predictive algorithm and the related monitor display. The research cockpit and video monitor was in a separate van. Altitude and airspeed were merged with the video signal onboard the model and overlaid onto the upper corners of the video image.

An initial longitudinal aerodynamic model of the Mothership was calculated using vortex-lattice techniques. Parameter estimation analysis of elevator doublet flight data was then used to update the initial model. A total of 28

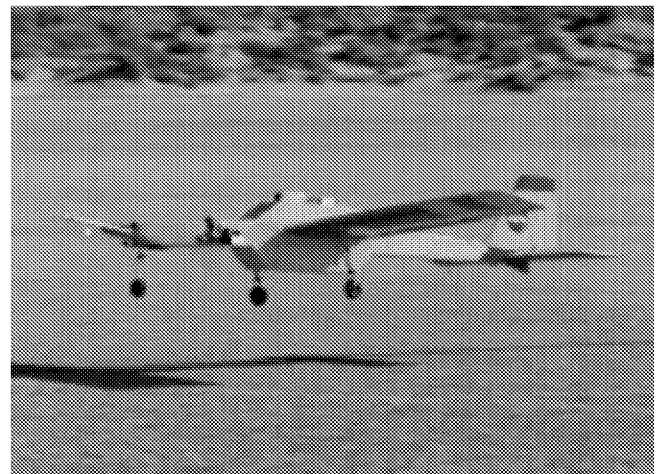
flights were flown for the initial functional checks and for parameter estimation.

The NASA model pilot, referred to as the "safety" pilot, stood outside of the van containing the ground cockpit. He was pilot in command and insured that the vehicle was kept within his visual range. He made all the takeoffs, landings, climbs, descent, and turns. On the straight leg of the flight pattern, he would give longitudinal stick and throttle control to the research pilot within the van. He could take back control at any time.

For the research flying of the program, 62 data sorties were flown over 16 test days for 20.5 hours of flight time. TPS was able to show that their model-based predictive algorithm improved handling qualities of the model flown as an UAV. With the predictor, the time delay tolerated was significantly increased. Or at the same time delay, pilot workload was significantly decreased. Including the initial checkout flights, a grand total of 90 flights were flown.

## Status/Plans

Dryden started in May, 1999. The research flight testing started in mid September and ended in mid October, 1999. USAF TPS technical report was finalized in December 1999. The successful completion of the program has potential to lead to a joint USAF/NASA program using a much larger vehicle.



Mothership Utility Model with 10 ft Wing Span

## Contacts

Alex Sim, DFRC, RA, (661) 258-3714

Tony Frackowiak, DFRC, AS&M, (661) 258-3473

Maj. Andrew Thurling, USAF TPS, (661) 277 3131

# HAVE RECKON Project

## Summary

When an Uninhabited Aerial Vehicle, UAV, is piloted from a ground control station, it is referred to as a Remotely Piloted Vehicle. A delay of typically 0.1 seconds is incurred as the vehicle processes the uplink signal and the vehicle response is prepared for downlink. When an RPV is flown over the horizon, the uplink and downlink signals still need to be relayed back to the ground station. A desirable relay is to use a satellite as the link. However a satellite link to the UAV and back often results in an additional signal transport delay of about 0.4 seconds. This 0.5 seconds total delay is enough to significantly degrade the handling qualities of an RPV. For a high-gain piloting task, this may even be enough lag to make the vehicle uncontrollable.

The USAF Test Pilot School, TPS, proposed to enhance the handling qualities by using a model-based predictive algorithm to compensate for system time delay. The algorithm would reside within the ground station and provide the ground pilot with predictive enhancements overlaid on the ground monitor. The compensation was functionally independent of the UAV. To conduct a low-cost flight research experiment, TPS contacted the Dryden Subscale Facility (model shop). Dryden agreed to provide the "UAV", safety pilot, ground cockpit, telemetry van and other lesser assets for the flight tests. The scope of the experiment was limited to the longitudinal axis.

## Objective

The USAF TPS general objective was to determine the improvement in UAV handling qualities when using a model-based predictive algorithm to compensate for system time delay. NASA Dryden's primary objectives were to provide the TPS with an aerodynamic model of the flight vehicle, integrate the vehicle systems, and safely conduct the flight tests.

## Results

Dryden chose a large utilitarian model, called the Mothership, that was capable of lifting 25 lbs of payload and still remain within the Dryden definition of a model airplane. A 16-channel data system was carried in a pod under the main fuselage. An airdata noseboom was mounted on the nose. A forward-looking video camera was installed in a pod above the wing. Measurements of elevator, pitch rate, and angle of attack were downlinked on the audio channel of the video signal. A telemetry van was used to separate the data from the audio channel and put it onto an ethernet line to an USAF Unix workstation next to the research cockpit. The workstation generated the transport lag by passing a delayed video frame to the monitor. The workstation was also used to generate the predictive algorithm and the related monitor display. The research cockpit and video monitor was in a separate van. Altitude and airspeed were merged with the video signal onboard the model and overlaid onto the upper corners of the video image.

An initial longitudinal aerodynamic model of the Mothership was calculated using vortex-lattice techniques. Parameter estimation analysis of elevator doublet flight data was then used to update the initial model. A total of 28

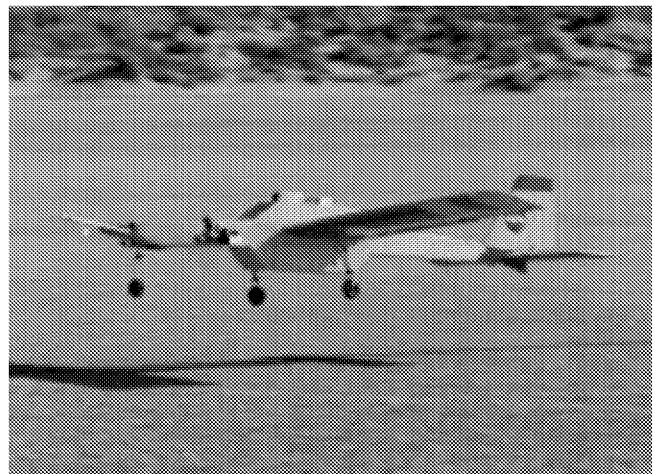
flights were flown for the initial functional checks and for parameter estimation.

The NASA model pilot, referred to as the "safety" pilot, stood outside of the van containing the ground cockpit. He was pilot in command and insured that the vehicle was kept within his visual range. He made all the takeoffs, landings, climbs, descent, and turns. On the straight leg of the flight pattern, he would give longitudinal stick and throttle control to the research pilot within the van. He could take back control at any time.

For the research flying of the program, 62 data sorties were flown over 16 test days for 20.5 hours of flight time. TPS was able to show that their model-based predictive algorithm improved handling qualities of the model flown as an UAV. With the predictor, the time delay tolerated was significantly increased. Or at the same time delay, pilot workload was significantly decreased. Including the initial checkout flights, a grand total of 90 flights were flown.

## Status/Plans

Dryden started in May, 1999. The research flight testing started in mid September and ended in mid October, 1999. USAF TPS technical report was finalized in December 1999. The successful completion of the program has potential to lead to a joint USAF/NASA program using a much larger vehicle.



Mothership Utility Model with 10 ft Wing Span

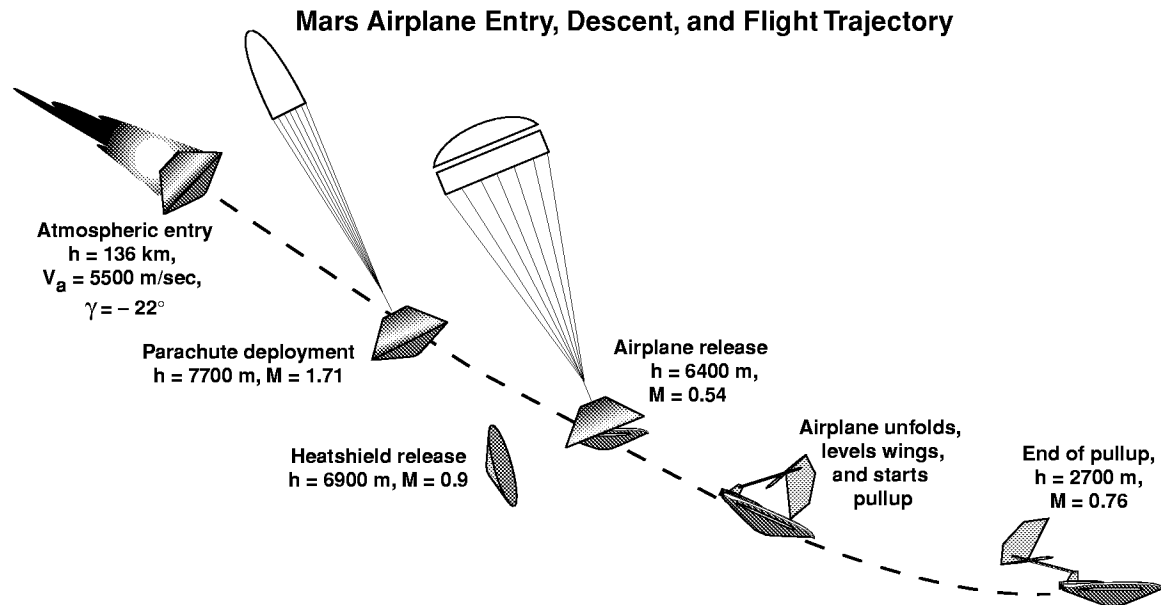
## Contacts

Alex Sim, DFRC, RA, (661) 258-3714

Tony Frackowiak, DFRC, AS&M, (661) 258-3473

Maj. Andrew Thurling, USAF TPS, (661) 277 3131

# Mars Airplane Entry, Descent and Flight Trajectory Development



## Summary

The Mars Airplane project was to provide the first opportunity for sustained lifting atmospheric flight on an interplanetary mission. For the mission, the aircraft is carried to the planet folded inside a small (75 cm diameter) aeroshell which makes a direct entry into the Martian atmosphere. Critical to the mission was the transition from the hypersonic, ballistic aeroshell to the subsonic lifting airplane. For initial design purposes a baseline Entry, Descent and Flight (EDF) trajectory profile was defined to consist of the following elements: ballistic entry of the aeroshell, supersonic deployment of a decelerator parachute, release of the heatshield, release, unfolding, and orientation of the airplane, and execution of a pullup maneuver to achieve trimmed, horizontal flight.

Given the predicted mass and aerodynamics of the aeroshell and airplane, and the predicted Martian atmospheric and topographical characteristics, a simulation of the EDF trajectory was built using the Program to Optimize Simulated Trajectories (POST). The trajectory optimization feature of POST was used to find the control strategy which maximized the surface-relative altitude of the airplane at the end of the pullup maneuver, subject to a number of design constraints.

## Objectives

The early development of a baseline (i. e. first-generation) EDF trajectory was important to provide the Mars Airplane design team with essential feedback early in the design cycle. The initial objective was to develop an EDF trajectory consistent with the baseline vehicle design data, and to optimize the trajectory within the allowable design space. With the optimal trajectory defined, the objective was to identify the sensitivity of the trajectory to design

parameter variations. A final objective was to use the results of sensitivity analysis to develop a second-generation control strategy.

## Results

For the baseline vehicle design, viable EDF trajectories were developed for sites in both the northern and southern hemispheres; altitudes at the end of the pullup maneuver were above 2 km. However, the high elevation of the desired science mission site (Parana Valles) precluded completion of the pullup maneuver before surface impact.

The performance metric (the surface-relative altitude at the end of the pullup maneuver) was a most sensitive to airplane mass, airplane lift and drag coefficients, and maximum Mach number allowed during the pullup. Not surprisingly, decreasing airplane mass, increasing lift coefficient, and increasing the allowable maximum Mach number yielded net altitude gains. Increasing the airplane drag coefficient to yield a net altitude increment. The performance metric showed only small sensitivity to other design parameter variations studied.

With the addition of airplane drag as a design variable, a second-generation control strategy showed that increasing drag significantly during the pullup maneuver yielded a net altitude increment of about 1.7 km.

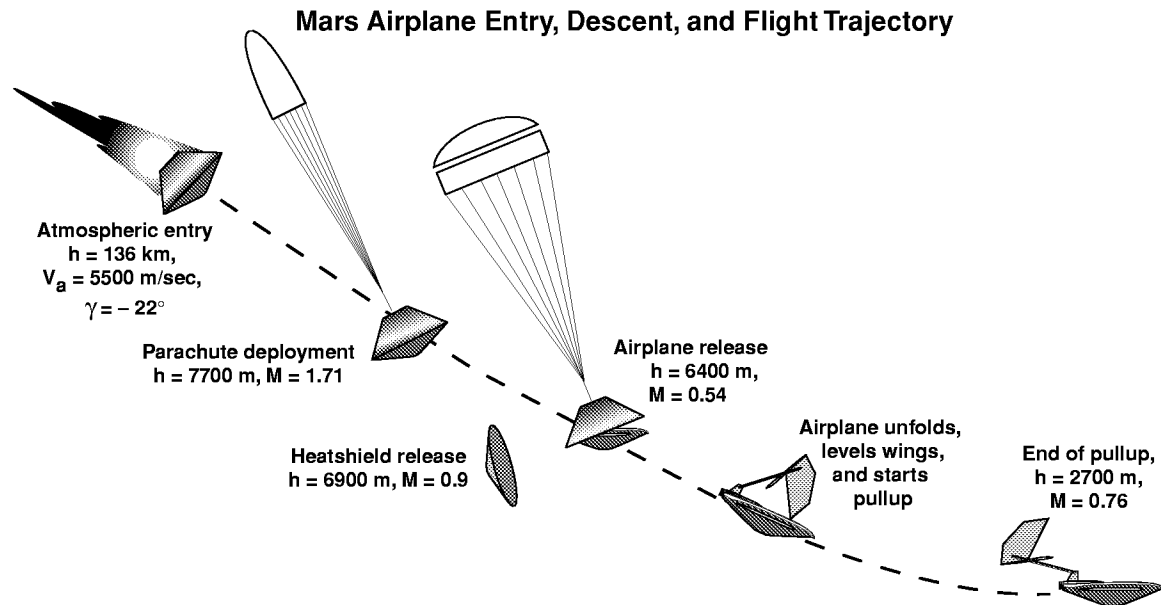
## Status/Plans

The Mars Airplane project was cancelled near the end of CY99. However, documentation of current results and some closeout work continues.

## Contacts

James Murray, DFRC, RA, (661) 258-2629  
Paul Tartabini, LaRC, (757) 864-787

# Mars Airplane Entry, Descent and Flight Trajectory Development



## Summary

The Mars Airplane project was to provide the first opportunity for sustained lifting atmospheric flight on an interplanetary mission. For the mission, the aircraft is carried to the planet folded inside a small (75 cm diameter) aeroshell which makes a direct entry into the Martian atmosphere. Critical to the mission was the transition from the hypersonic, ballistic aeroshell to the subsonic lifting airplane. For initial design purposes a baseline Entry, Descent and Flight (EDF) trajectory profile was defined to consist of the following elements: ballistic entry of the aeroshell, supersonic deployment of a decelerator parachute, release of the heatshield, release, unfolding, and orientation of the airplane, and execution of a pullup maneuver to achieve trimmed, horizontal flight.

Given the predicted mass and aerodynamics of the aeroshell and airplane, and the predicted Martian atmospheric and topographical characteristics, a simulation of the EDF trajectory was built using the Program to Optimize Simulated Trajectories (POST). The trajectory optimization feature of POST was used to find the control strategy which maximized the surface-relative altitude of the airplane at the end of the pullup maneuver, subject to a number of design constraints.

## Objectives

The early development of a baseline (i. e. first-generation) EDF trajectory was important to provide the Mars Airplane design team with essential feedback early in the design cycle. The initial objective was to develop an EDF trajectory consistent with the baseline vehicle design data, and to optimize the trajectory within the allowable design space. With the optimal trajectory defined, the objective was to identify the sensitivity of the trajectory to design

parameter variations. A final objective was to use the results of sensitivity analysis to develop a second-generation control strategy.

## Results

For the baseline vehicle design, viable EDF trajectories were developed for sites in both the northern and southern hemispheres; altitudes at the end of the pullup maneuver were above 2 km. However, the high elevation of the desired science mission site (Parana Valles) precluded completion of the pullup maneuver before surface impact.

The performance metric (the surface-relative altitude at the end of the pullup maneuver) was a most sensitive to airplane mass, airplane lift and drag coefficients, and maximum Mach number allowed during the pullup. Not surprisingly, decreasing airplane mass, increasing lift coefficient, and increasing the allowable maximum Mach number yielded net altitude gains. Increasing the airplane drag coefficient to yield a net altitude increment. The performance metric showed only small sensitivity to other design parameter variations studied.

With the addition of airplane drag as a design variable, a second-generation control strategy showed that increasing drag significantly during the pullup maneuver yielded a net altitude increment of about 1.7 km.

## Status/Plans

The Mars Airplane project was cancelled near the end of CY99. However, documentation of current results and some closeout work continues.

## Contacts

James Murray, DFRC, RA, (661) 258-2629  
Paul Tartabini, LaRC, (757) 864-787

# Blunt Body Drag Reduction Using Forebody Surface Roughness

## Introduction

Current proposed shapes for trans-atmospheric launch and crew-return vehicles like the X-33, X-34, X-38, and "Venture-Star" have extremely large base areas when compared to previous hypersonic vehicle designs. As a result, base drag - especially in the transonic flight regime -- is expected to be very large. The unique configuration of the X-33, with its very large base area and relatively low forebody drag, offers the potential for a very high payoff in overall performance if the base drag can be reduced significantly.

## Drag Reduction Strategy

For blunt-based objects whose base areas are heavily separated, a clear relationship between the base drag and the "viscous" forebody drag has been demonstrated (ref. 1, 2). (Figure 1) As the forebody drag is increased; generally the base drag of the projectile tends to decrease. This base-drag reduction is a result of boundary layer effects at the base of the vehicle. The shear layer caused by the free-stream flow rubbing against the dead, separated air in the base region acts as a jet pump and serves to reduce the pressure coefficient in the base areas. The surface boundary layer acts as an "insulator" between the external flow and the dead air at the base. As the forebody drag is increased, the boundary layer thickness at the aft end of the forebody increases, -- reducing the effectiveness of the pumping mechanism - - and the base drag is reduced.

Configurations with large base drag coefficients, necessarily lie on the steep portion of the curve a small increment in the forebody friction drag should result in a relatively large decrease in the base drag. Conceptually, if the added increment in forebody skin drag is optimized with respect to the base drag reduction, then it may be possible to reduce the *overall drag of the configuration*.

## The LASRE Drag Reduction Experiment

The LASRE experiment (ref. 3) was a flight test of a roughly 20% half-span model of an X-33 forebody with a single aerospike rocket engine at the rear. The entire test model is mounted on top of a SR-71 aircraft. In order to measure performance of the Linear Aerospike engine under a variety of flight conditions, the model was mounted to the SR-71 with a pylon which was instrumented with 8 load-cells oriented to allow a six-degree-of-freedom measurement of the total forces and moments. The model was also instrumented with surface pressure ports that allowed the model profile drag to be measured by numerically integrating the surface pressure distributions.

The LASRE drag reduction experiment sought to increase the forebody skin friction and modify the boundary layer at the back end of the LASRE model. Clearly, one of the most convenient methods of increasing the forebody skin drag is to add roughness to the surface. LASRE results verified that as the forebody drag is increased; generally the base drag of the projectile tends to decrease. LASRE tests verified that this drag reduction persists through transonic and well into the supersonic flight regime. Pre-flight analyses predicted that a trade off of viscous forebody drag to base drag may make it possible to achieve a net drag reduction by adding roughness to the forebody skin.

Unfortunately, even though the LASRE experiments demonstrated a strong base drag reduction effect; the net drag was not reduced. The roughened forebody caused the forebody pressures to rise and offset the base drag benefits, which were gained. At this time it is unclear whether this forebody pressure rise was a fault of the manner in which the forebody grit was applied, or whether it is even possible to achieve a net drag reduction. Further tests, under a more controlled flow environment, must be conducted to resolve this uncertainty.

# Blunt Body Drag Reduction Using Forebody Surface Roughness

## Introduction

Current proposed shapes for trans-atmospheric launch and crew-return vehicles like the X-33, X-34, X-38, and "Venture-Star" have extremely large base areas when compared to previous hypersonic vehicle designs. As a result, base drag - especially in the transonic flight regime -- is expected to be very large. The unique configuration of the X-33, with its very large base area and relatively low forebody drag, offers the potential for a very high payoff in overall performance if the base drag can be reduced significantly.

## Drag Reduction Strategy

For blunt-based objects whose base areas are heavily separated, a clear relationship between the base drag and the "viscous" forebody drag has been demonstrated (ref. 1, 2). (Figure 1) As the forebody drag is increased; generally the base drag of the projectile tends to decrease. This base-drag reduction is a result of boundary layer effects at the base of the vehicle. The shear layer caused by the free-stream flow rubbing against the dead, separated air in the base region acts as a jet pump and serves to reduce the pressure coefficient in the base areas. The surface boundary layer acts as an "insulator" between the external flow and the dead air at the base. As the forebody drag is increased, the boundary layer thickness at the aft end of the forebody increases, -- reducing the effectiveness of the pumping mechanism - - and the base drag is reduced.

Configurations with large base drag coefficients, necessarily lie on the steep portion of the curve a small increment in the forebody friction drag should result in a relatively large decrease in the base drag. Conceptually, if the added increment in forebody skin drag is optimized with respect to the base drag reduction, then it may be possible to reduce the *overall drag of the configuration*.

## The LASRE Drag Reduction Experiment

The LASRE experiment (ref. 3) was a flight test of a roughly 20% half-span model of an X-33 forebody with a single aerospike rocket engine at the rear. The entire test model is mounted on top of a SR-71 aircraft. In order to measure performance of the Linear Aerospike engine under a variety of flight conditions, the model was mounted to the SR-71 with a pylon which was instrumented with 8 load-cells oriented to allow a six-degree-of-freedom measurement of the total forces and moments. The model was also instrumented with surface pressure ports that allowed the model profile drag to be measured by numerically integrating the surface pressure distributions.

The LASRE drag reduction experiment sought to increase the forebody skin friction and modify the boundary layer at the back end of the LASRE model. Clearly, one of the most convenient methods of increasing the forebody skin drag is to add roughness to the surface. LASRE results verified that as the forebody drag is increased; generally the base drag of the projectile tends to decrease. LASRE tests verified that this drag reduction persists through transonic and well into the supersonic flight regime. Pre-flight analyses predicted that a trade off of viscous forebody drag to base drag may make it possible to achieve a net drag reduction by adding roughness to the forebody skin.

Unfortunately, even though the LASRE experiments demonstrated a strong base drag reduction effect; the net drag was not reduced. The roughened forebody caused the forebody pressures to rise and offset the base drag benefits, which were gained. At this time it is unclear whether this forebody pressure rise was a fault of the manner in which the forebody grit was applied, or whether it is even possible to achieve a net drag reduction. Further tests, under a more controlled flow environment, must be conducted to resolve this uncertainty.



# Blunt Body Drag Reduction Using Forebody Surface Roughness

**Wind Tunnel Tests** A series of low-speed wind tunnel tests is currently being conducted to prove the existence of this elusive Drag Bucket. In these tests a two-dimensional cylinder with a blunt after body is being tested (Figure 2). For the simple 2-D tests total body force measurements will be determined by numerically integrating surface pressures and by skin drag calculations made using the boundary layer velocity profile measurements. High-frequency wake pressure (Strouhal number) measurements will also be obtained. By adding micro-machined surface overlays (Figure 3) to increase the surface roughness it is hoped that the overall drag of the configurations can be reduced. The predicted drag reduction is shown in figure 4. The body flow characteristics predicted by CFD analyses are shown in figure 5. The trailing Von-Karman "vortex-street" wake is clearly visible. Significant instrumentation system development was achieved during FY '99. Test results confirming these predictions should be available by mid year FY '00.

## References

- 1) Hoerner, Sighard F., *Fluid Dynamic Drag*, Self-Published Work, Library of Congress Card Number 64-19666, Washington, D.C., 1965, pp. 3-19, 3-20, 15-4, 16-5.
- 2) Saltzman, Edwin J., Wang, Charles K., and Iliff, Kenneth W., *Flight Determined Subsonic Lift and Drag Characteristics of Seven Blunt-Based Lifting-Body and Wing-Body Reentry Vehicle Configurations*, AIAA Paper # 99-0383, 1999.
- 1) Whitmore, Stephen A., and Moes, Timothy R., *A Base Drag Reduction Methods on the X-33 Linear Aerospike SR-71 Experiment (LASRE) Flight Program*, AIAA 99-0277, January 1999.

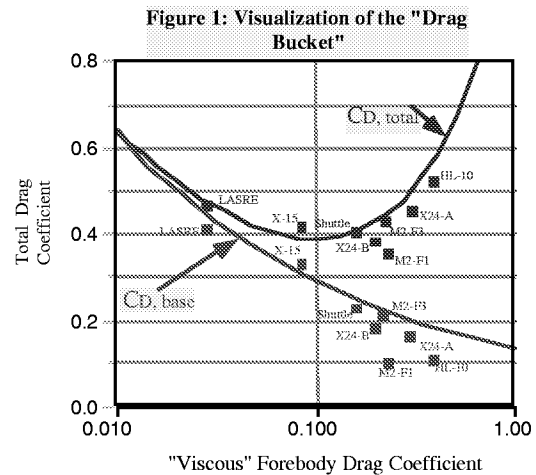


Figure 2: Wind Tunnel Model for Base Drag / Forebody-Roughness Study:

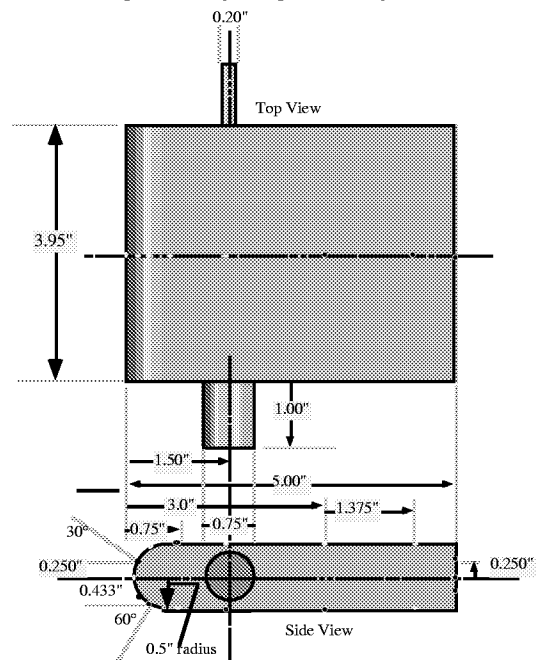
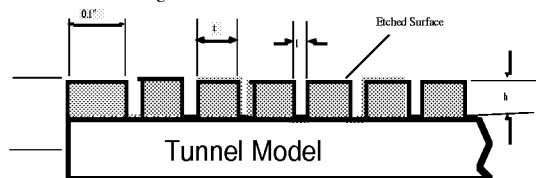


Figure 3: Inset of Bar Grid Pattern



# Blunt Body Drag Reduction Using Forebody Surface Roughness

**Wind Tunnel Tests** A series of low-speed wind tunnel tests is currently being conducted to prove the existence of this elusive Drag Bucket. In these tests a two-dimensional cylinder with a blunt after body is being tested (Figure 2). For the simple 2-D tests total body force measurements will be determined by numerically integrating surface pressures and by skin drag calculations made using the boundary layer velocity profile measurements. High-frequency wake pressure (Strouhal number) measurements will also be obtained. By adding micro-machined surface overlays (Figure 3) to increase the surface roughness it is hoped that the overall drag of the configurations can be reduced. The predicted drag reduction is shown in figure 4. The body flow characteristics predicted by CFD analyses are shown in figure 5. The trailing Von-Karman "vortex-street" wake is clearly visible. Significant instrumentation system development was achieved during FY '99. Test results confirming these predictions should be available by mid year FY '00.

## References

- 1) Hoerner, Sighard F., *Fluid Dynamic Drag*, Self-Published Work, Library of Congress Card Number 64-19666, Washington, D.C., 1965, pp. 3-19, 3-20, 15-4, 16-5.
- 2) Saltzman, Edwin J., Wang, Charles K., and Iliff, Kenneth W., *Flight Determined Subsonic Lift and Drag Characteristics of Seven Blunt-Based Lifting-Body and Wing-Body Reentry Vehicle Configurations*, AIAA Paper # 99-0383, 1999.
- 1) Whitmore, Stephen A., and Moes, Timothy R., *A Base Drag Reduction Methods on the X-33 Linear Aerospike SR-71 Experiment (LASRE) Flight Program*, AIAA 99-0277, January 1999.

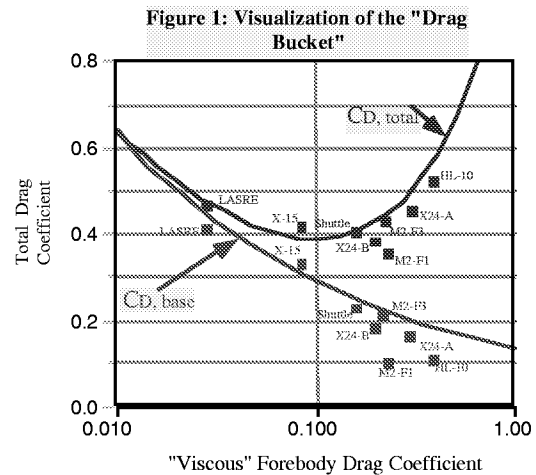


Figure 2: Wind Tunnel Model for Base Drag / Forebody-Roughness Study:

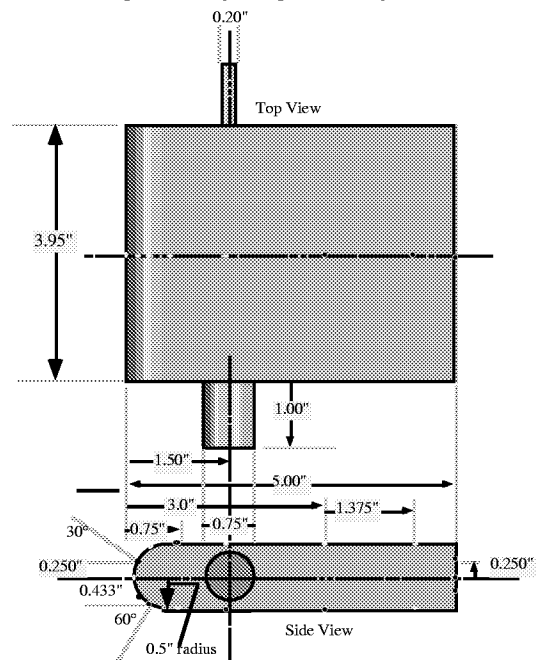
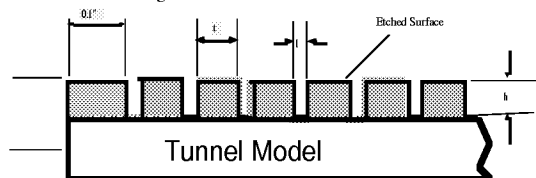


Figure 3: Inset of Bar Grid Pattern



# Blunt Body Drag Reduction Using Forebody Surface Roughness

Table I: "Bar-Grid" Roughness Dimensions  
(See Inset Diagram) ( $K_s \sim$  Equivalent Sand Grain Roughness of Plate)

0.0020	0.0020	0.0020	0.0064	± .0005	
0.0020	0.0040	0.0020	0.0114	± .0005	
0.0020	0.0060	0.0050	0.0206	± .0005	
0.0050	0.0120	0.0050	0.0330	± .0010	
0.0100	0.0150	0.0100	0.0450	± .0010	
0.0100	0.0200	0.0100	0.0570	± .0010	
0.0200	0.0400	0.0200	0.1140	± .0015	
0.0200	0.0800	0.0200	0.1911	± .0015	
0.0400	0.1000	0.0400	0.2721	± .0020	
0.0400	0.1500	0.0400	0.3660	± .0020	

Figure 4: Predicted Drag Reduction for Wind Tunnel Model

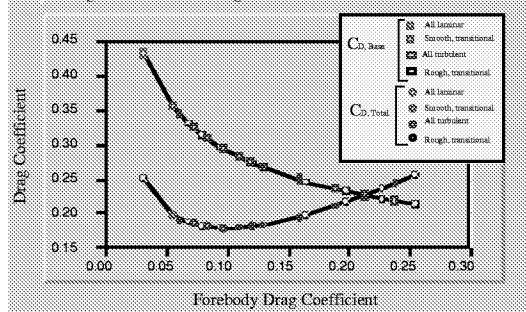
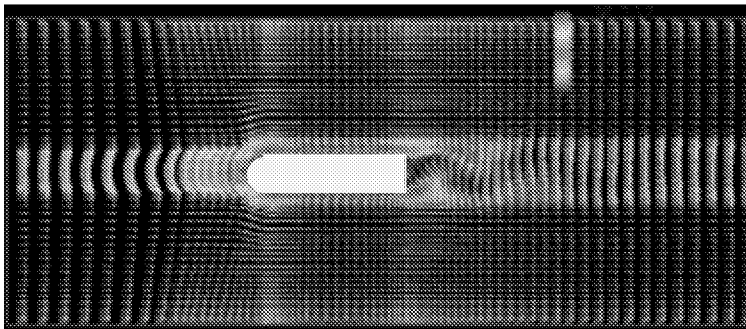



Figure 5: CFD Results for Wind Tunnel Model Showing Von-Karman



0.0020	0.0020	0.0020	0.0064	$\pm .0005$
0.0020	0.0040	0.0020	0.0114	$\pm .0005$
0.0020	0.0060	0.0050	0.0206	$\pm .0005$
0.0050	0.0120	0.0050	0.0330	$\pm .0010$
0.0100	0.0150	0.0100	0.0450	$\pm .0010$
0.0100	0.0200	0.0100	0.0570	$\pm .0010$
0.0200	0.0400	0.0200	0.1140	$\pm .0015$
0.0200	0.0800	0.0200	0.1911	$\pm .0015$
0.0400	0.1000	0.0400	0.2721	$\pm .0020$
0.0400	0.1500	0.0400	0.3660	$\pm .0020$

Figure 10 is a scatter plot showing the relationship between the Drag Coefficient (y-axis) and the Forebody Drag Coefficient (x-axis). The y-axis ranges from 0.15 to 0.45, and the x-axis ranges from 0.00 to 0.30. The plot displays two main data series:  $C_{D, \text{base}}$  and  $C_{D, \text{Total}}$ . Each series is further divided into three sub-series based on the flow regime: All laminar (represented by open symbols), Smooth, transitional (represented by half-filled symbols), and All turbulent (represented by filled symbols). The  $C_{D, \text{base}}$  series shows a decreasing trend as the Forebody Drag Coefficient increases, while the  $C_{D, \text{Total}}$  series shows a more complex, non-monotonic relationship.

Forebody Drag Coefficient	$C_{D, \text{base}}$ (All laminar)	$C_{D, \text{base}}$ (Smooth, transitional)	$C_{D, \text{base}}$ (All turbulent)	$C_{D, \text{Total}}$ (All laminar)	$C_{D, \text{Total}}$ (Smooth, transitional)	$C_{D, \text{Total}}$ (All turbulent)
0.04	0.43	0.43	0.43	0.25	0.25	0.25
0.08	0.35	0.35	0.35	0.19	0.19	0.19
0.12	0.29	0.29	0.29	0.18	0.18	0.18
0.16	0.26	0.26	0.26	0.19	0.19	0.19
0.20	0.23	0.23	0.23	0.22	0.22	0.22
0.24	0.21	0.21	0.21	0.23	0.23	0.23
0.26	0.21	0.21	0.21	0.25	0.25	0.25



# DC-8 Reduced Vertical Separation Minimum (RVSM) Certification

## Summary

The NASA Dryden DC-8 Airborne Science Laboratory (N817NA) performs research around the globe, recently in support of the SAGE III Ozone Loss and Validation Experiment (SOLVE). This experiment utilized a large region of airspace, the North Atlantic (NAT) airspace corridor, which is subject to Reduced Vertical Separation Minimum (RVSM) requirements. These requirements allow aircraft traffic to be separated by 1,000 feet vertically between 29,000 and 41,000 feet MSL, as compared to the usual 2,000 feet separation. RVSM non-group aircraft compliance requires  $\pm 160$  feet pressure altitude accuracy. RVSM allows greater traffic density while maintaining safe aircraft separation.

A commercial service for RVSM certification was considered, but involved significant modification to the aircraft, high cost, and an unacceptable schedule impact to Airborne Science research commitments. The approach taken was done internally with insignificant aircraft modification, minimal cost, and little schedule impact.

## Objective

Obtain RVSM certification through an airdata calibration of the DC-8 static pressure system achieving  $\pm 160$  feet accuracy.

## Approach

RVSM quality airdata computers were installed in the aircraft, and these data were recorded using the DC-8's Data Acquisition and Distribution System (DADS). These airdata computers have a worst case avionics error of 85 feet after 24 months. For the calibration flights a carrier-phase differential global positioning system (DGPS) receiver and antenna was employed. The DGPS gave geometric altitude of the aircraft to an accuracy better than 2 feet. A pressure calibration of the atmosphere on flight test days was determined by data from a network of rawinsonde weather balloons, synoptic analysis, and surface observations.

By combining DGPS geometric altitude with the pressure calibration of the atmosphere, the true pressure altitude of the aircraft is determined. This is compared to the airdata computer measurement with no error corrections to determine the static source error correction (SSEC) required to null the pressure altitude errors. The SSEC for both the pilot and co-pilot systems were then incorporated into the airdata computers, and checked on a verification flight. The SSEC is a function only of Mach number.

The DC-8 was flown near maximum speed (Mach 0.48 to 0.54) at 500 feet above Rogers Dry Lakebed in steady flight. These data gave the SSEC with minimal uncertainty of the atmospheric pressure calibration. Most of the flight data was taken at 29,000 to 41,000 feet in stabilized flight between Mach 0.51 and 0.86. The near-ground data were used to adjust the high altitude data for small temperature biases on the rawinsonde balloons. DGPS data taken during constant airspeed turns were used to measure winds independent of the rawinsonde balloons.

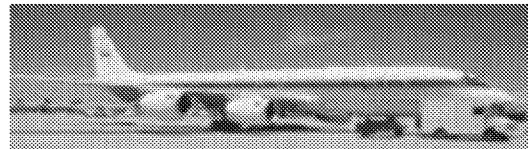
Autopilot operation was verified during stabilized flight to conform to the  $\pm 65$  feet RVSM requirement.

## Results

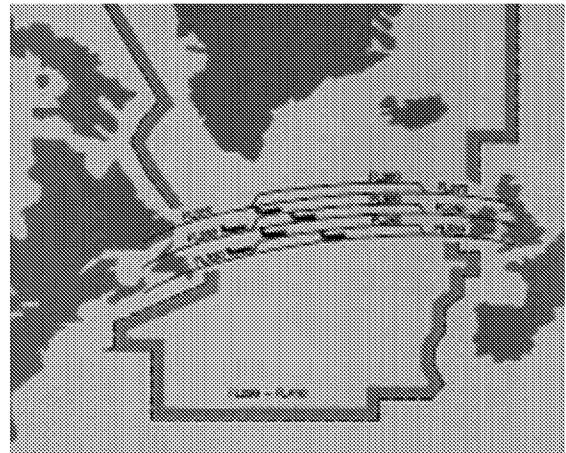
One calibration flight was flown to determine the SSEC required to null pressure altitude errors with the aircraft in a clean configuration. These data yielded error residuals of  $\pm 15$  feet for both the pilot and co-pilot static pressure system.

A verification flight was performed with a variety of airborne science probes external to the aircraft, including a large nacelle about 5 feet from the static pressure ports. This constituted a worst case scenario of possible SSEC shifts. The maximum residual error on this flight was 73 feet, and when combined with the worst case avionics error of 85 feet and the DGPS accuracy of 2 feet gives a total error of 160 feet, just meeting the RVSM requirement. The errors would be considerably less if the airborne science probe near the static ports is removed or relocated. Autopilot operation was demonstrated to be within  $\pm 30$  feet.

RVSM certification was granted on November 18, 1999.



DC-8 Airborne Science Laboratory (N817NA)



Current RVSM airspace in North Atlantic

## Contacts

Edward A. Haering, Jr., DFRC, RA, (661) 258-3696

Edward H. Teets, Jr., DFRC, RA, (661) 258-2924

David A. Webber, DFRC, OE, (661) 258-7541

# DC-8 Reduced Vertical Separation Minimum (RVSM) Certification

## Summary

The NASA Dryden DC-8 Airborne Science Laboratory (N817NA) performs research around the globe, recently in support of the SAGE III Ozone Loss and Validation Experiment (SOLVE). This experiment utilized a large region of airspace, the North Atlantic (NAT) airspace corridor, which is subject to Reduced Vertical Separation Minimum (RVSM) requirements. These requirements allow aircraft traffic to be separated by 1,000 feet vertically between 29,000 and 41,000 feet MSL, as compared to the usual 2,000 feet separation. RVSM non-group aircraft compliance requires  $\pm 160$  feet pressure altitude accuracy. RVSM allows greater traffic density while maintaining safe aircraft separation.

A commercial service for RVSM certification was considered, but involved significant modification to the aircraft, high cost, and an unacceptable schedule impact to Airborne Science research commitments. The approach taken was done internally with insignificant aircraft modification, minimal cost, and little schedule impact.

## Objective

Obtain RVSM certification through an airdata calibration of the DC-8 static pressure system achieving  $\pm 160$  feet accuracy.

## Approach

RVSM quality airdata computers were installed in the aircraft, and these data were recorded using the DC-8's Data Acquisition and Distribution System (DADS). These airdata computers have a worst case avionics error of 85 feet after 24 months. For the calibration flights a carrier-phase differential global positioning system (DGPS) receiver and antenna was employed. The DGPS gave geometric altitude of the aircraft to an accuracy better than 2 feet. A pressure calibration of the atmosphere on flight test days was determined by data from a network of rawinsonde weather balloons, synoptic analysis, and surface observations.

By combining DGPS geometric altitude with the pressure calibration of the atmosphere, the true pressure altitude of the aircraft is determined. This is compared to the airdata computer measurement with no error corrections to determine the static source error correction (SSEC) required to null the pressure altitude errors. The SSEC for both the pilot and co-pilot systems were then incorporated into the airdata computers, and checked on a verification flight. The SSEC is a function only of Mach number.

The DC-8 was flown near maximum speed (Mach 0.48 to 0.54) at 500 feet above Rogers Dry Lakebed in steady flight. These data gave the SSEC with minimal uncertainty of the atmospheric pressure calibration. Most of the flight data was taken at 29,000 to 41,000 feet in stabilized flight between Mach 0.51 and 0.86. The near-ground data were used to adjust the high altitude data for small temperature biases on the rawinsonde balloons. DGPS data taken during constant airspeed turns were used to measure winds independent of the rawinsonde balloons.

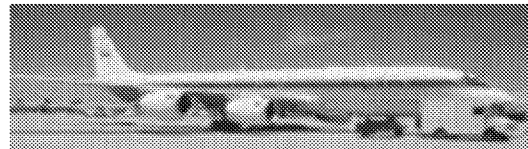
Autopilot operation was verified during stabilized flight to conform to the  $\pm 65$  feet RVSM requirement.

## Results

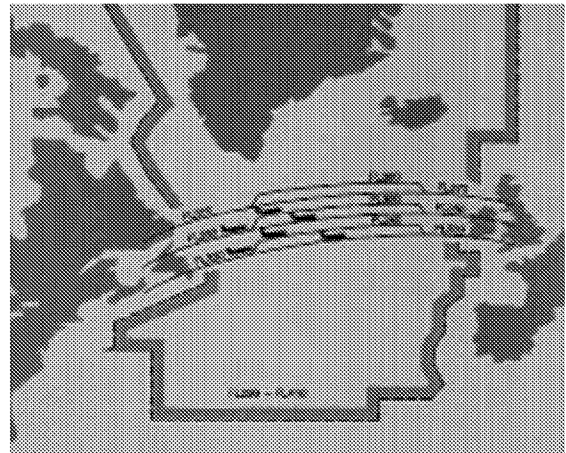
One calibration flight was flown to determine the SSEC required to null pressure altitude errors with the aircraft in a clean configuration. These data yielded error residuals of  $\pm 15$  feet for both the pilot and co-pilot static pressure system.

A verification flight was performed with a variety of airborne science probes external to the aircraft, including a large nacelle about 5 feet from the static pressure ports. This constituted a worst case scenario of possible SSEC shifts. The maximum residual error on this flight was 73 feet, and when combined with the worst case avionics error of 85 feet and the DGPS accuracy of 2 feet gives a total error of 160 feet, just meeting the RVSM requirement. The errors would be considerably less if the airborne science probe near the static ports is removed or relocated. Autopilot operation was demonstrated to be within  $\pm 30$  feet.

RVSM certification was granted on November 18, 1999.



DC-8 Airborne Science Laboratory (N817NA)



Current RVSM airspace in North Atlantic

## Contacts

Edward A. Haering, Jr., DFRC, RA, (661) 258-3696

Edward H. Teets, Jr., DFRC, RA, (661) 258-2924

David A. Webber, DFRC, OE, (661) 258-7541

# F-18 Stability and Control Derivative Estimation for Active Aeroelastic Wing Risk Reduction

## Summary

The NASA Dryden F-18 System Research Aircraft (SRA) was used to obtain stability and control derivatives from flight data for a baseline F-18 aircraft. This work was done at the higher dynamic pressure range of the F-18 envelope in support of a future F-18 program known as Active Aeroelastic Wing (AAW). The AAW technology integrates vehicle aerodynamics, active controls, and structural aeroelastic behavior to maximize vehicle performance. In particular, the goal of the AAW project will be to maximize the contribution of a reduced-stiffness F-18A wing to roll rate performance. In order to support the technology, changes to flight control computers and software will be required and therefore a good understanding of the basic F-18 individual control surface effectiveness is essential. The SRA was used to provide that understanding.

## Objective

The primary objective of this program was to obtain detailed understanding of the effectiveness of each control surface at the various test conditions. The results can then be used to update the aerodynamic model for the F-18 and therefore improve the effectiveness of the control laws being developed for the AAW aircraft.

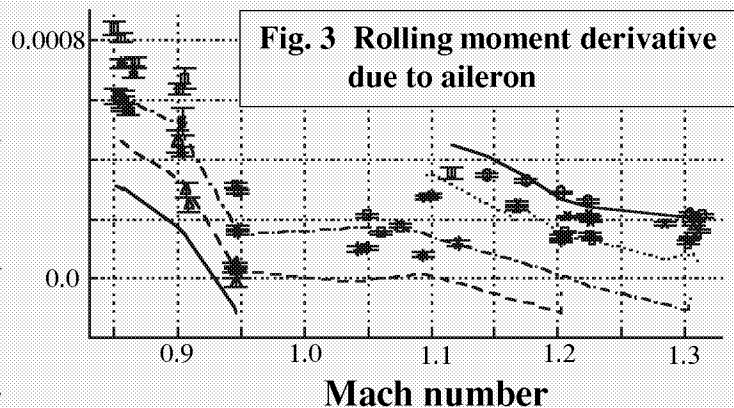
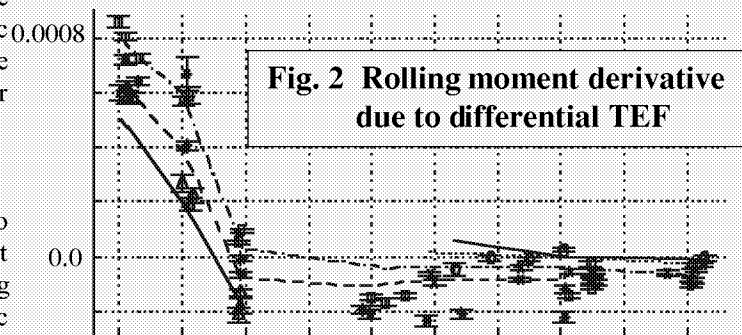
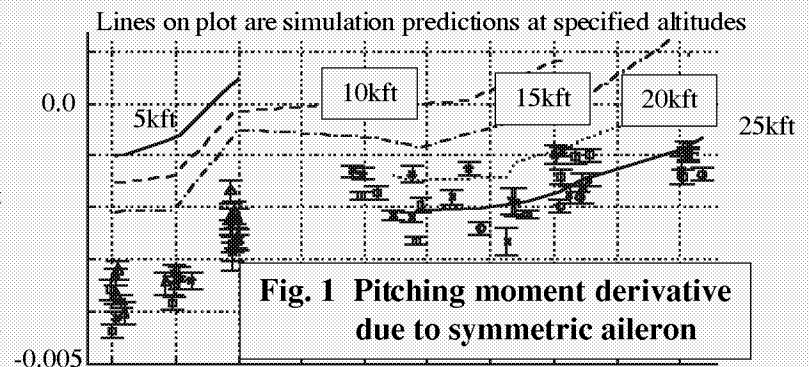
## Approach

An on-board excitation system (OBES) was used to provide uncorrelated single surface input (SSI) doublet sequences. Longitudinal maneuvers included leading edge flap (LEF), trailing edge flap (TEF), symmetric aileron, and symmetric horizontal tail SSIs. Lateral-directional maneuvers include rudder, differential LEF, differential TEF, aileron, and differential tail SSIs. The pilot would initiate the maneuver sequence from the cockpit and the OBES would command the SSI doublets. In some cases, the surfaces were moved in combinations which are not used by the basic F-18 control laws. These included symmetric LEF, TEF, and aileron deflections at high speeds. Data was analyzed post-flight using an output-error parameter estimation algorithm.

## Results

A complete set of stability and control derivatives has been obtained for 20 different Mach/Altitude test conditions. The effect of symmetric aileron deflection on pitching moment is shown in figure 1. As can be seen, the flight determined results (symbols) show that there is more pitching moment effectiveness than

predicted by the simulation (especially at subsonic Mach numbers). Control surface rolling moment "reversal" was of special interest to the project. Figures 2 and 3 show TEF and aileron rolling moment derivatives. As seen in figure 2, TEF reversal was measured in flight at Mach 0.95 for altitudes below 10,000 ft. Aileron reversal was not measured in flight (figure 3), but reduced aileron effectiveness was clearly seen as the subsonic Mach number increased and altitude decreased.



## Status

The results of this study are being used to update the F-18 aerodynamic model for simulation use AAW control law development.

## Contacts

Tim Moes, DFRC, RA, (661) 258-3054  
Greg Noffz, DFRC, RA, (661) 258-2417  
(NASA TM currently in production)

# F-18 Stability and Control Derivative Estimation for Active Aeroelastic Wing Risk Reduction

## Summary

The NASA Dryden F-18 System Research Aircraft (SRA) was used to obtain stability and control derivatives from flight data for a baseline F-18 aircraft. This work was done at the higher dynamic pressure range of the F-18 envelope in support of a future F-18 program known as Active Aeroelastic Wing (AAW). The AAW technology integrates vehicle aerodynamics, active controls, and structural aeroelastic behavior to maximize vehicle performance. In particular, the goal of the AAW project will be to maximize the contribution of a reduced-stiffness F-18A wing to roll rate performance. In order to support the technology, changes to flight control computers and software will be required and therefore a good understanding of the basic F-18 individual control surface effectiveness is essential. The SRA was used to provide that understanding.

## Objective

The primary objective of this program was to obtain detailed understanding of the effectiveness of each control surface at the various test conditions. The results can then be used to update the aerodynamic model for the F-18 and therefore improve the effectiveness of the control laws being developed for the AAW aircraft.

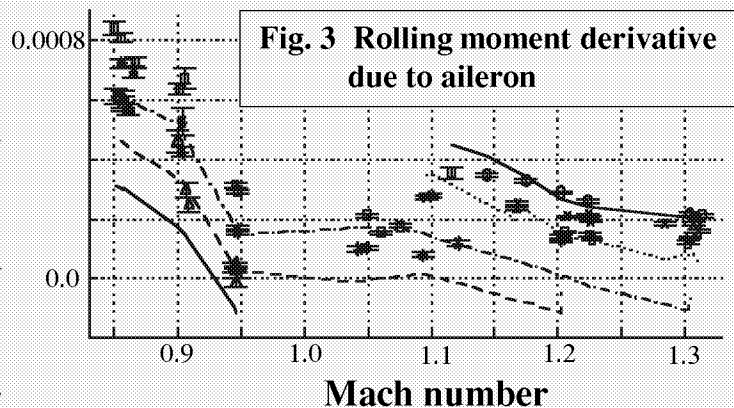
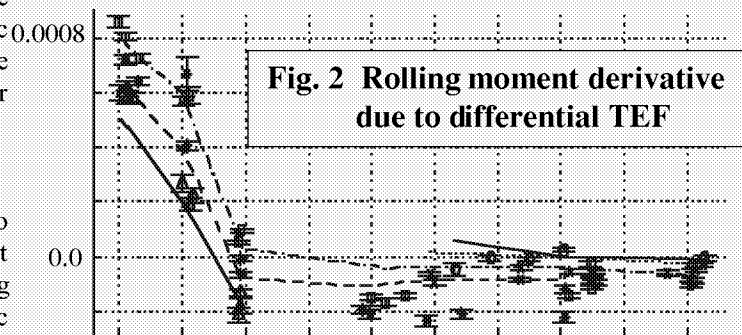
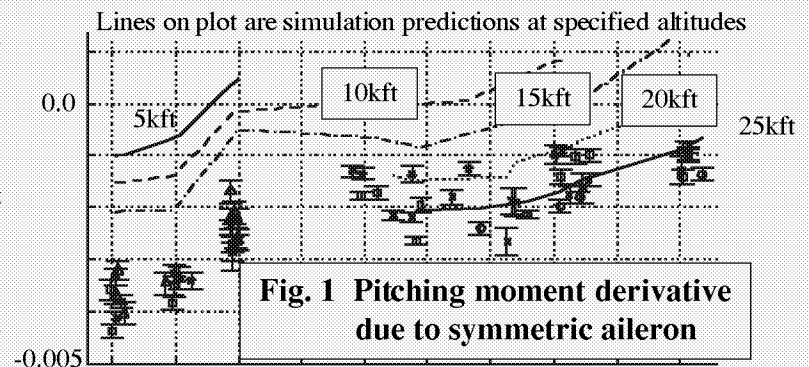
## Approach

An on-board excitation system (OBES) was used to provide uncorrelated single surface input (SSI) doublet sequences. Longitudinal maneuvers included leading edge flap (LEF), trailing edge flap (TEF), symmetric aileron, and symmetric horizontal tail SSIs. Lateral-directional maneuvers include rudder, differential LEF, differential TEF, aileron, and differential tail SSIs. The pilot would initiate the maneuver sequence from the cockpit and the OBES would command the SSI doublets. In some cases, the surfaces were moved in combinations which are not used by the basic F-18 control laws. These included symmetric LEF, TEF, and aileron deflections at high speeds. Data was analyzed post-flight using an output-error parameter estimation algorithm.

## Results

A complete set of stability and control derivatives has been obtained for 20 different Mach/Altitude test conditions. The effect of symmetric aileron deflection on pitching moment is shown in figure 1. As can be seen, the flight determined results (symbols) show that there is more pitching moment effectiveness than

predicted by the simulation (especially at subsonic Mach numbers). Control surface rolling moment "reversal" was of special interest to the project. Figures 2 and 3 show TEF and aileron rolling moment derivatives. As seen in figure 2, TEF reversal was measured in flight at Mach 0.95 for altitudes below 10,000 ft. Aileron reversal was not measured in flight (figure 3), but reduced aileron effectiveness was clearly seen as the subsonic Mach number increased and altitude decreased.



## Status

The results of this study are being used to update the F-18 aerodynamic model for simulation use AAW control law development.

## Contacts

Tim Moes, DFRC, RA, (661) 258-3054  
Greg Noffz, DFRC, RA, (661) 258-2417  
(NASA TM currently in production)



# SR-71 Testbed Configuration Envelope Expansion

## Summary

A four flight envelope expansion program was conducted on NASA Dryden's SR-71A aircraft in the "Testbed" configuration. This configuration included a large "canoe-like" structure and reflection plane mounted on top of the SR-71 as seen in figure 1. This structure was previously used to carry the Linear Aerospike SR-71 Experiment (LASRE). Widespread interest has been expressed in using the testbed configuration for flight test of various propulsion and aerodynamic experiments at Mach numbers of up to 3.2. Consequently, NASA conducted the envelope expansion test program to look at the configuration performance, thermal environment, and stability and control (S&C).

## Objective

Demonstrate maximum performance and stability and control characteristics of the SR-71 testbed configuration.

## Approach

The approach was to incrementally build up Mach number on each flight. Longitudinal and lateral-directional doublets were flown at various Mach/Altitude conditions to obtain the S&C data. A post-flight output-error parameter estimation algorithm was used to obtain S&C derivatives.

## Results

### Performance:

The added aerodynamic drag of an experiment is most critical in the transonic acceleration, where excess thrust is at a minimum. Poor transonic acceleration can affect the maximum Mach number attainable since less fuel is available for the acceleration. On "hot" days, i.e. the temperature versus altitude profile is well above the Standard Day profile, the SR-71 J58 engine thrust is significantly reduced, thereby significantly reducing the maximum Mach capability. The SR-71 Test Bed configuration successfully reached Mach 3.0 on a "hot" day. Analysis has shown that Mach 3.2 is attainable, however, flight demonstration of this was not accomplished due to an in-flight system failure. The previous LASRE program reached a maximum Mach of 1.8 in flight. Analysis showed that the LASRE configuration could have achieved Mach 2.5 for a standard day temperature profile. The additional drag due to the part of the LASRE experiment located above the reflection plane is shown in figure 2. Future experiments desiring Mach numbers greater than 2.5 need to have drag increments less than that shown in figure 2.

## Stability and Control

The largest S&C concern for the testbed configuration was reduced direction stability,  $C_{nb}$ . Figure 3 shows the flight determined  $C_{nb}$  values for the baseline and testbed SR-71 configuration. At Mach 2.1 the testbed configuration showed a steep decline in open-loop directional stability.  $C_{nb}$  did, however, remain positive up through Mach 3.0. The closed-loop directional stability provided by the stability augmentation system (SAS) was significantly better due to side acceleration feedback. Piloted simulations of engine unstart events were done that showed that the configuration was safe to fly with the reduced stability.

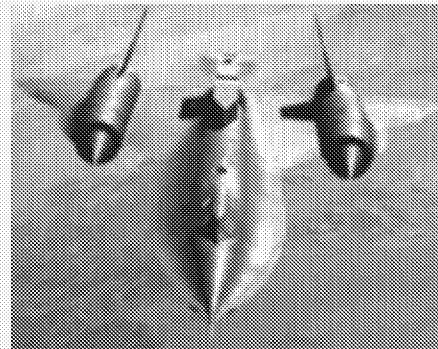


Fig. 1 - SR-71 Testbed configuration.

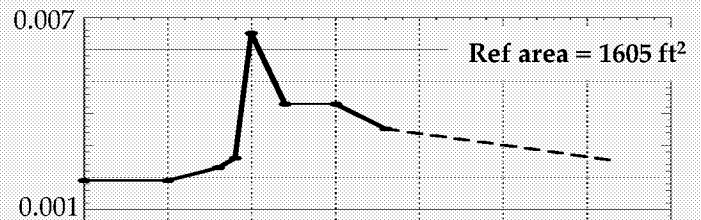


Fig. 2 - Drag coefficient due to LASRE experiment

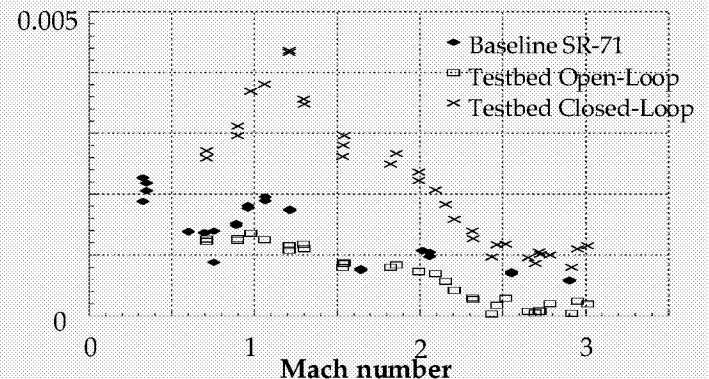


Fig. 3 - Directional Stability Coefficient

## Status

The SR-71 testbed is capable for flight testing new aerodynamic and propulsion experiments at Mach numbers up to 3.2

## Contacts

Tim Moes, DFRC, RA, (661) 258-3054  
Stephen Corda, DFRC, RP, (661) 258-2103  
(NASA TM currently in production)

# SR-71 Testbed Configuration Envelope Expansion

## Summary

A four flight envelope expansion program was conducted on NASA Dryden's SR-71A aircraft in the "Testbed" configuration. This configuration included a large "canoe-like" structure and reflection plane mounted on top of the SR-71 as seen in figure 1. This structure was previously used to carry the Linear Aerospike SR-71 Experiment (LASRE). Widespread interest has been expressed in using the testbed configuration for flight test of various propulsion and aerodynamic experiments at Mach numbers of up to 3.2. Consequently, NASA conducted the envelope expansion test program to look at the configuration performance, thermal environment, and stability and control (S&C).

## Objective

Demonstrate maximum performance and stability and control characteristics of the SR-71 testbed configuration.

## Approach

The approach was to incrementally build up Mach number on each flight. Longitudinal and lateral-directional doublets were flown at various Mach/Altitude conditions to obtain the S&C data. A post-flight output-error parameter estimation algorithm was used to obtain S&C derivatives.

## Results

### Performance:

The added aerodynamic drag of an experiment is most critical in the transonic acceleration, where excess thrust is at a minimum. Poor transonic acceleration can affect the maximum Mach number attainable since less fuel is available for the acceleration. On "hot" days, i.e. the temperature versus altitude profile is well above the Standard Day profile, the SR-71 J58 engine thrust is significantly reduced, thereby significantly reducing the maximum Mach capability. The SR-71 Test Bed configuration successfully reached Mach 3.0 on a "hot" day. Analysis has shown that Mach 3.2 is attainable, however, flight demonstration of this was not accomplished due to an in-flight system failure. The previous LASRE program reached a maximum Mach of 1.8 in flight. Analysis showed that the LASRE configuration could have achieved Mach 2.5 for a standard day temperature profile. The additional drag due to the part of the LASRE experiment located above the reflection plane is shown in figure 2. Future experiments desiring Mach numbers greater than 2.5 need to have drag increments less than that shown in figure 2.

## Stability and Control

The largest S&C concern for the testbed configuration was reduced direction stability,  $C_{nb}$ . Figure 3 shows the flight determined  $C_{nb}$  values for the baseline and testbed SR-71 configuration. At Mach 2.1 the testbed configuration showed a steep decline in open-loop directional stability.  $C_{nb}$  did, however, remain positive up through Mach 3.0. The closed-loop directional stability provided by the stability augmentation system (SAS) was significantly better due to side acceleration feedback. Piloted simulations of engine unstart events were done that showed that the configuration was safe to fly with the reduced stability.

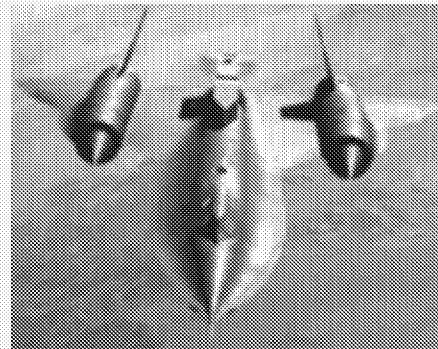


Fig. 1 - SR-71 Testbed configuration.

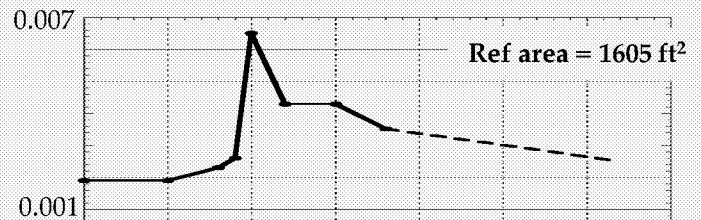


Fig. 2 - Drag coefficient due to LASRE experiment

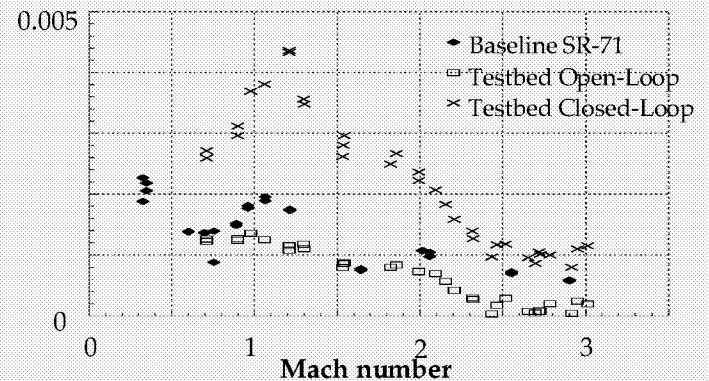


Fig. 3 - Directional Stability Coefficient

## Status

The SR-71 testbed is capable for flight testing new aerodynamic and propulsion experiments at Mach numbers up to 3.2

## Contacts

Tim Moes, DFRC, RA, (661) 258-3054  
Stephen Corda, DFRC, RP, (661) 258-2103  
(NASA TM currently in production)

# Flight Test of a Gripen Ministick Controller in an F/A-18 Aircraft

## Summary

In March of 1999 five pilots conducted a handling qualities evaluation in an F/A-18 research aircraft of the small displacement center stick controller developed for by Sweden for the JAS-39 Gripen. The Production Support Flight Control Computers (PSFCC) provided the interface between the controller hardware installed in the aft cockpit and the standard flight control laws for the F/A-18 aircraft.

## Objective

The primary objective of the flight research program was to assess any changes in the handling qualities of the F/A-18 aircraft as a result of the mechanical characteristics of the ministick. The secondary objective was a demonstration of the capability of the PSFCC to support flight test experiments.

## Approach

The ministick controller and demodulator box output single channel pitch and roll stick commands. These DC signals were input into the PSFCC analog inputs. Software was developed to perform cross-channel data links, signal selection and command scaling. The signals were scaled to be similar to the maximum inputs of the standard F/A-18 control stick. Because the experiment was to assess the effects of the mechanical characteristics of a small displacement center mounted control stick, the original software deadbands and stick shaping were used.

A five flight test program was conducted using five pilots. General comments and handling qualities ratings were collected. The flight testing consisted of the following maneuvers: doublets, frequency sweeps, bank attitude captures, pitch attitude captures, echelon formation flight, column formation flight, gross acquisition, and fine tracking. There were three phases to the echelon formation: gentle maneuvering, vertical

captures and more aggressive maneuvering. The three phases for column formation flight were: gentle maneuvering, more aggressive maneuvering, and lateral captures.

## Results

Cooper Harper ratings from the pilots are summarized in the table below. The pilot comments consistently noted that the stick was very sensitive in roll with some tendency to ratcheting. This could be mitigated by modifying the stick shaping and deadband. The general pilots comments on the stick were favorable. It was noted that it was extremely easy to put in full amplitude inputs.

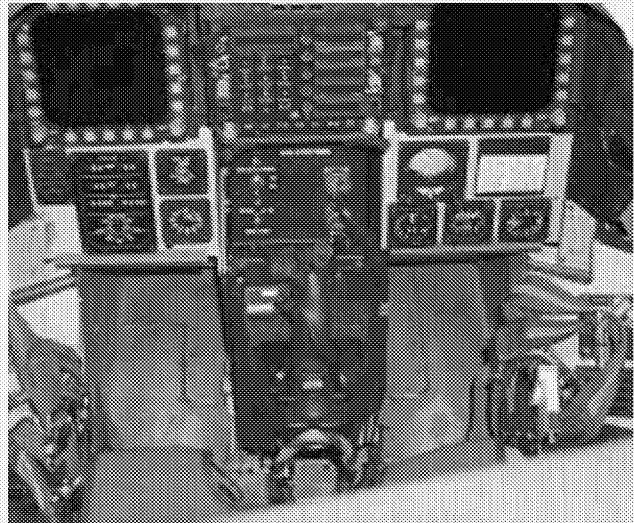
## Status

Data analysis is being completed and a technical reports are being prepared to document the flight test, compare results with handling qualities criteria, and to describe the PSFCC implementation and testing process.

## Contacts

Patrick C. Stoliker, DFRC, RC, (661) 258-2706

John Carter, DFRC, RC, (661) 258-2025



Ministick installed in the aft cockpit of an F-18

Pilot	A	B	C	D	E
Echelon Formation Phase 1	4	3	2	3	3
Echelon Formation Phase 2	4	5	3	2	4
Echelon Formation Phase 3	4 to 7	5	4	4	5
Column Formation Phase 1	4	3	2	4	4
Column Formation Phase 2	3	3	2	4	5
Column Formation Phase 3	3 to 4	5	5	4	4
Gross Acquisition	n/a	6 to 7	2	2	4
Longitudinal Fine Tracking	n/a	3	2	2	3
Lateral Fine Tracking	n/a	4	2	3	6

Summary of pilot ratings

# Flight Test of a Gripen Ministick Controller in an F/A-18 Aircraft

## Summary

In March of 1999 five pilots conducted a handling qualities evaluation in an F/A-18 research aircraft of the small displacement center stick controller developed for by Sweden for the JAS-39 Gripen. The Production Support Flight Control Computers (PSFCC) provided the interface between the controller hardware installed in the aft cockpit and the standard flight control laws for the F/A-18 aircraft.

## Objective

The primary objective of the flight research program was to assess any changes in the handling qualities of the F/A-18 aircraft as a result of the mechanical characteristics of the ministick. The secondary objective was a demonstration of the capability of the PSFCC to support flight test experiments.

## Approach

The ministick controller and demodulator box output single channel pitch and roll stick commands. These DC signals were input into the PSFCC analog inputs. Software was developed to perform cross-channel data links, signal selection and command scaling. The signals were scaled to be similar to the maximum inputs of the standard F/A-18 control stick. Because the experiment was to assess the effects of the mechanical characteristics of a small displacement center mounted control stick, the original software deadbands and stick shaping were used.

A five flight test program was conducted using five pilots. General comments and handling qualities ratings were collected. The flight testing consisted of the following maneuvers: doublets, frequency sweeps, bank attitude captures, pitch attitude captures, echelon formation flight, column formation flight, gross acquisition, and fine tracking. There were three phases to the echelon formation: gentle maneuvering, vertical

captures and more aggressive maneuvering. The three phases for column formation flight were: gentle maneuvering, more aggressive maneuvering, and lateral captures.

## Results

Cooper Harper ratings from the pilots are summarized in the table below. The pilot comments consistently noted that the stick was very sensitive in roll with some tendency to ratcheting. This could be mitigated by modifying the stick shaping and deadband. The general pilots comments on the stick were favorable. It was noted that it was extremely easy to put in full amplitude inputs.

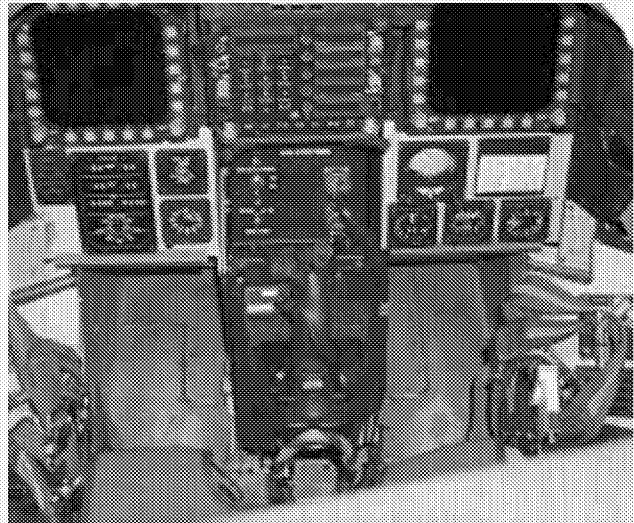
## Status

Data analysis is being completed and a technical reports are being prepared to document the flight test, compare results with handling qualities criteria, and to describe the PSFCC implementation and testing process.

## Contacts

Patrick C. Stoliker, DFRC, RC, (661) 258-2706

John Carter, DFRC, RC, (661) 258-2025



Ministick installed in the aft cockpit of an F-18

Pilot	A	B	C	D	E
Echelon Formation Phase 1	4	3	2	3	3
Echelon Formation Phase 2	4	5	3	2	4
Echelon Formation Phase 3	4 to 7	5	4	4	5
Column Formation Phase 1	4	3	2	4	4
Column Formation Phase 2	3	3	2	4	5
Column Formation Phase 3	3 to 4	5	5	4	4
Gross Acquisition	n/a	6 to 7	2	2	4
Longitudinal Fine Tracking	n/a	3	2	2	3
Lateral Fine Tracking	n/a	4	2	3	6

Summary of pilot ratings